ADDIS ABABA UNIVERSITY

SCHOOL OF GRADUATE STUDIES

INTEGRATED GEOPHYSICAL INVESTIGATIONS TO CHARACTERIZE THE SHASHAMANE-AJE 2016 GROUND FISSURES, MAIN ETHIOPIAN RIFT

By:

Mekdes Samuel

A THESIS SUBMITTED TO THE SCHOOL OF GRADAUTE STUDIES OF ADDIS ABABA UNIVERSITY IN PARTILA FULFILMENT OF THE REQUIREMENTS FOR THE DEGREE OF MASTYER OF SCIENCE IN GEOPHYSICS

May 2017

ADDIS ABABA UNIVERSITY

SCHOOL OF GRADUATE STUDIES

INTEGRATED GEOPHYSICAL INVESTIGATIONS TO CHARACTERIZE THE SHASHAMANE-AJE 2016 GROUND FISSURES, MAIN ETHIOPIAN RIFT

By:

Mekdes Samuel

Signed by the Examining and Graduate Committee:

Dr. Balemwal Atnafu: Signature----------Date----------
Chairman of School Graduate Committee

Prof. Tigistu Haile: Signature----------Date----------
Advisor

Dr. Getnet Mewa: Signature----------Date----------
Examiner

.

Dr. Shimeles Fisseha: Signature----------Date----------
Examiner

ACKNOWLEDGEMENT

I have no words to say to my advisor Prof. Tigistu Haile for the proper supervision, support and guidance he provided me throughout my research. His critical comments, fatherly approach and unreserved effort have given me the opportunity to explore more. I sincerely appreciate his patience and willingness to devote much of his time and energy at all stages of my work. I would like to say thank you for flowered project that covers all the field work budgets.

I thank Dr. Getenet Mewa, Dr. Tilahun Azagegn, Dr. Bekele Abebe and Dr. Abera Alemu for their contributions on my research work.

I would like to thank also the PhD. students Addis Eshetu and Assefa Getaneh for their support to use Geosoft Oasis Montaj software in the processing of the geophysical data.

I thank also to all my family and friends for their support and encouragement during the period of this work.

Table of Contents **Page**

List of Figures **Page**

ABSTRACT

In this thesis work two integrated geophysical methods, namely magnetic and electrical resistivity (resistivity sounding and axial Dipole-Dipole profiling) have been carried out over the large size ground fissure that occurred following the heavy inundation in the summer of 2016 at Oine Chafo Umbure, Shashamane area which is located within the Central part of the Main Ethiopian Rift (CMER).

The electrical data were then analyzed and interpreted with appropriate software and presented in the form of apparent resistivity pseudodepth and geoelectric section as well and 2D inverse model sections for the Dipole-Dipole survey. The pseudodepth section shows that the shallow zones (approximately up to depth of 50m) have high resistivity and the extensive substratum part have low resistivity values. The geoelectric section constructed for the same profile shows that the subsurface consists of 4 geoelectric horizons. The 2D inverse model section of the two Dipole-Dipole profiles show that there are three subsurface horizons up to the depth of 18m with some layer discontinuities. The top and bottom layers have high resistivity while the intermediate horizon has moderate to low resistivity.

The magnetic data were corrected and the resulting anomaly plots are presented in terms of residual plots and analytic signal maps. The residual magnetic profile values were also modeled to obtain possible subsurface stratification of the area. Interpretation of magnetic data and the 2D magnetic model section both show that there are a number of discontinuities transecting the area around the fissures. The combined geophysical survey result shows that the low resistivity second layer is the weakest layer on the subsurface that resulted in sliding of the top layers and formation of the fissures due to excessive clogging with the water. It was no, however, possible

to correlate the various discontinuities mapped with the survey to the deeper Rift structures because of the limitation of the depth of investigation of the electrical surveys.

CHAPTER ONE

INTRODUCTION

1.1 Background

The Main Ethiopian Rift is the northern terminus of the East African Rift system (EARS). It is a magmatic rift that records all the different stages of rift evolution from rift initiation to break-up and embryonic oceanic spreading. The central part of this Rift system as it passes over Ethiopia forms what is called the Main Ethiopian Rift (MER) which is an ideal place to analyze the evolution of continental extension, the rupture of lithospheric plates and the dynamics by which distributed continental deformation is progressively focused at oceanic spreading centers (Corti, 2009).

The MER at its narrowest section is some 80km wide while, most tectonic and volcanic activities are concentrated with in a10–20km wide sub-axial zone known as the Wonji Fault Belt (WFB). This is not a continuous belt but is formed of a series of offset segments, each consisting of short and often closely spaced normal faults and fissures arranged en echelon form (Ameha A. Muluneh et al., 2014). Although the component segments of the Wonji Fault Belt are oriented more or less parallel to the rift margins, the faults themselves generally are not. Their orientation ranges from about N40˚ E to N–S. A series of Quaternary volcanoes occur along the belt, often located at these offsets. These volcanoes are composed mainly of trachytes and rhyolites and some have collapsed into summit calderas which are linked to voluminous ash flow tuffs. These, together with lacustrine sediments, volcanic ash fall deposits and fissure basalts form the covering of the rift floor (Corti, 2009).

The floor of the Rift has been recently found to exhibit a number of ground fissures that are extensive in nature and form in a more or less aligned trend with the Wonji Fault Belt system. These ground fissures are long, linear tensile structures that are visible at the land surface with or without vertical offsets.

Ground fissures can take place as a result of two possible causes: the first one is due to human interference (man-made actions) which imposes direct impact on subsurface formations while

the second one is due to natural causes. Some man-made activities could cause these cracks. Removal of a large block of the earth crust or deep excavations is an example of human interference. Withdrawal of ground water and oil or any of soil components could cause enormous damage and initiate cracks. Cracks occurring due to the impact of nature without human interference can be divided into two parts. The first part is directly linked to tectonic activities and the second part is linked to melting and decomposition of soil either chemically or physically when exposed to water (Fouzan et al., 2014).

Among the causes and mechanisms through which ground cracks can be formed, the most ones are related to geological, hydrological and geomorphological anomalies whereas immediate triggers are usually rainfall and earthquakes. Geological anomalies include strong lithological, structural and weathering heterogeneities, buried faults, scarps and bedrock highs, soluble rocks and organic soils. Hydrological problems, on the other hand, are often related to a decline in groundwater level and the subsequent adjustment in aquifer systems, while topography plays an important role since ground cracks are usually reported to occur in basins, valleys and volcanic depressions (Lulseged Ayalew et al., 2004).

In the summer of 2015-16 during the month of July, a number of ground cracks have formed at different places within the rift floor. Some of the prominent cracks occurred near Weyo and Abosa townships (both on and adjacent to the Addis Ababa- Aawassa main road), Muleti area on the south western side of Lake Aawassa and on the main road between Shashamane and Aje town. Of these affected areas, the large ground crack that formed close to Shashamane town (at specific place of Oine Chafo Umbure) are the most remarkable in their extent and the large mass of material removed cutting the road section and affecting transportation and extensive damage caused to the farm lands adjoining the road (Figures 1.1 (a) and (b)). The crack occurred a few hours following the heavy rains in the area and the strong run off coming from Shashamane town following the main asphalted road drainage and culverts.

Integrated geophysical methods, namely electrical resistivity and magnetic methods would be used in order to study the fissures and possibly to identify the reasons that led to the emergence of such phenomena of considerable extent in an area close to Shashamane town.

The magnetic method is use to identify geologic structures in the area that could be associated with pre and post fissure activity. The resistivity method, on the other hand, is use to investigate the vertical and lateral resistivity variations of the different layers and to determine vertical and lateral extent of the fissures by making pseudo sections and geoelectric sections from the combined VES data and dipole-dipole resistivity profiling data.

Figure 1.1. (a).The Ground fissures that developed at Oine Chafo Umbure on the Shashamane-Aje road in the summer of 2016 and in (b) is old asphalt road in the foreground.

This research work is therefore targeted at using geophysical techniques as tools for understanding the nature (geometry, extent, depth…) and possible cause for the occurrence of the ground cracks.

Based on the interpretation of the results obtained after applying these methods, information on possible causes and the overall areal extent of the fissures is to be expected. Also the future status of the area in relation to exposures to similar events especially in relation to the farm lands of the area is expected be known. These results are very important for the community that live in the area and for others that use the asphalt road which is one of the main roads connecting the rift floor town with the towns in southwest of Ethiopia.

1.2 Location of Study Area

The study area is located at the central part of Main Ethiopian Rift. It is located on the asphalt road between Shashamane and Aje at specific place called Oine Chafo Umbure (Figure 1.2). The specific coordinates of the survey location; easting is 450575 to 451196 and northing 798189 to 798836 with elevation ranging between 1818 to 1826m above mean sea level. The area is of a flat topography with extensive agricultural activity and a number of villages surround the sides of the main asphalt road. In terms of geology, the area is mainly covered by tuff, ignimbrite and pumice.

1.3 Statement of the Problem

Earth fissures have suddenly appeared in the area around Oine Chafo Umbure, Shashamane severely damaging the asphalt road and large parts of agricultural lands, i.e. the affected area is mainly used for transportation (asphalt road) and agriculture. The unexpected appearance of the Earth fissure, in addition to disrupting the heavy traffic to the major cities and towns south west of the country, caused insecurity among the farmers and people in the area due to concern that a huge portion of the farm lands will be rendered unusable and the fissures might interfere with future land use in the area. This project work will attempt to examine the underlying cause of the fissure and to recommend solutions to mitigate the problem.

.

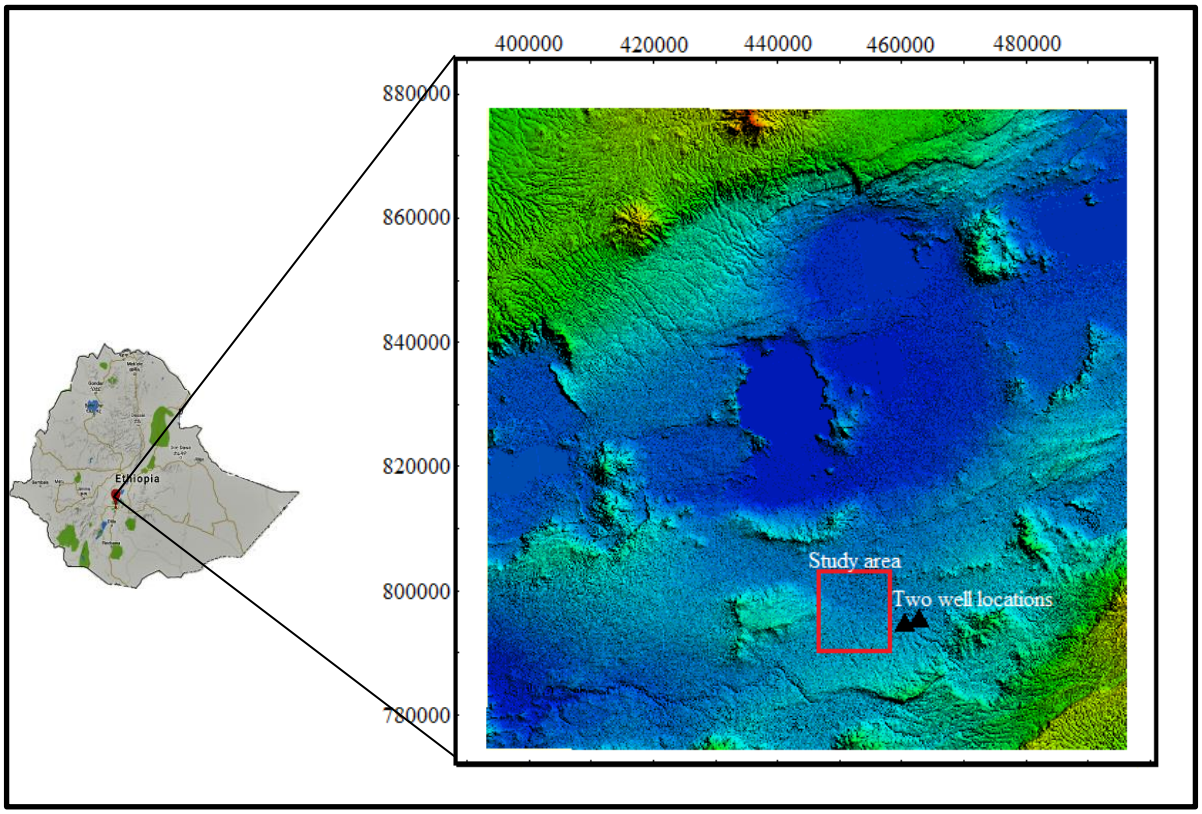

Figure 1.2. Location map of the study area with the region marked with a rectangle showing the specific area of study.

1.4 Objective

1.4.1 General objective

The main objective of this study is to understand the cause and areal extent of the ground fissure that occurred in the summer of 2015/16 around Oine Chafo umbure.

1.4.2 Specific objectives

- To establish the vertical and lateral electrical/lithological stratification of the area.
- To determine the depth, lateral and horizontal extent of the ground fissures and its relation to Rift geological structures.
- To investigate/identify/shade light on the possible causes and mechanisms for the ground fissures.
- To know the feasibility of the study area in relation to its use for future large structure (roads, buildings, etc.) construction.

1.5 Previous Works

Since the study area is part of the Main Ethiopian Rift which is very vulnerable to ground cracking, a number of researches associated with ground cracks and fissures have been conducted. The most significant ones are discussed below.

Ground fissures problem were common in many parts of world. In most parts, it can be caused by land subsidence effect as result of high ground water removal as reported by many researchers. There is also a case many ground cracks propagate upward from the subsurface and the surface expression of an opening is the last result of the release in accumulated strain.

According to (Lulseged Ayalew et al., 2004) there is no accurate relation between ground crack in Ethiopian rift valley with aquifer system compaction and increased horizontal seepage stress. This is due to the fact that the level of groundwater withdrawal responsible for these processes is still negligible in Ethiopia. Also ground crack appeared have no direct link with active faulting or distant earth quakes. However, a seismic elastic strain, which originates at depth and propagates up ward through sediments without the formation of bed rock faults, could result in conditions conducive to the development of cracks. Then, fissures might ultimately be created after heavy rainfalls by near-surface processes such as piping and hydro compaction along water-line sources.

LaikeMariam Asfaw (1998) summarized about 12 fissures reported in the Main Ethiopian Rift between 1956 and 1996. They occur in the thick unconsolidated lacustrine and volcanic sediments which covers the rift floor. In all cases reported, the fissures were orientated generally in the direction of the rift. In almost all cases they were revealed as a result of sub-surface erosion and consequent slumping following heavy rains.

In one case sedimentary fissures have been directly related to earthquake swarms in the northern part of the MER (LaikeMariam Asfaw, 1982). The development of such earthquake-induced sedimentary fissures has been shown to have the morphology of subsidence pits connected by cracks.

A study of the distribution of sedimentary fissures with relation to the geology and hydrogeology of the MER shows that all the sites of reported sedimentary fissures occur in the same geological formations. However, reports of sedimentary fissures in the rift are not uniformly distributed over such geological formations. In particular, when such geological formations occur in arid regions, corresponding reports of sedimentary fissures do not exist. Furthermore, the sudden manifestation of sedimentary fissures in relation to rainfall implies that rainfall is an important factor in the realization of sedimentary fissures. From the mean annual rainfall distribution for the region is clear that all the sites reported to date are in areas with a mean annual rainfall of 400 mm or more. When the rainfall is below 400 mm, sedimentary fissures have not been reported (Laikemariam Asfaw, 1998)

It must be noted here that geology, hydrogeology and rainfall have been used as variables in characterizing the occurrence of sedimentary fissures in the MER.

Based on the hydrogeological map of the region shows that the flow direction of groundwater in the region does not correlate with the orientation of reported fissures . Where subsurface flows have been reported following the occurrence of fissures, these must have created a conduit different in direction from that of the regional groundwater flow. Rather than the groundwater flow direction, the orientation of the fissures correlates strongly with the direction of the rift axis.

Williams et al., 2003 describes a swarm of tensional fissures located at the northern end of main Ethiopian rift that related to the age of rift widening and occurs at welded tuff. As suggested the fissures appeared to be tensional features.

1.6 Methodology

In this research work, two geophysical methods were used, namely electrical resistivity and magnetic methods. The electrical resistivity survey consisted of both sounding and profiling surveys while the magnetic method used magnetic profiling survey. In general, the Dipole-Dipole survey traverses and magnetic survey traverses were selected so as to cross the ground

fissure and its possible extension on either side and in a direction perpendicular to the fissure orientation whereas the VES profile is selected parallel to the strike of the ground crack.

The Electrical Resistivity method to be utilized would be composed of Dipole-Dipole Resistivity profiling and Vertical Electrical Sounding (VES) surveys. Dipole-Dipole Resistivity profiling would be carried out to know both the lateral and vertical variation in ground apparent resistivity to a limited depth (because of the available instrumentation). The VES surveys on the other hand are expected to give a 1-D vertical probing of the subsurface to a relatively larger depth.

VES survey were conducted at 3 sounding points using the Schlumberger array with a maximum half-electrode spacing of 500m (i.e. AB/2=500m). The electrical profiling survey on the other hand, was conducted along 2 lines at the two ends of the fissure with one line on either side of the fissures. The profiling surveys were carried out at 10m inter electrode spacing with the Axial Dipole-Dipole arrangement over six slices/ depth sections. It is seen that with this procedure, the arrangement mapped the subsurface to a depth of about 18m. Both profiling and VES surveys were carried out with the IRIS Syscal R1 Plus Swith 72 system.

The magnetic profiling, on the other hand, were conducted over 6 selected traverse lines with line spacing of 50m and station spacing 10m.

1.7 Data Presentation and Interpretation

The electrical VES data will be presented in terms of interpreted individual VES, apparent resistivity pseudodepth and geoelectric sections, while the Dipole-Dipole data yielding 2D inverse resistivity model sections. These representations of the electrical data were then subjected to interpretation in terms of the objectives of the survey.

The corrected magnetic data were presented as magnetic profiles, contour maps and model sections. The magnetic profiles were qualitatively interpreted by visual inspection as well as quantitatively using the model sections.

1.8 Application of Results

The result of this work is useful to understand the main causes of the problem of ground fissures in the area and if possible suggest measures that will help the community and governmental organizations to take measures to minimize the risks caused by similar problems.

The result mainly helps the peoples that live in the area and farmers to protect themselves from similar hazards by implementing remedial measures in land use, surface water run off management, etc.

The results of the work are expected to be used as inputs

- for people in the locality of the fissures who lost a considerable portion of their farm land to the fissures in terms of understanding future possible similar fissures,
- for people that use the asphalt roads for transportation,
- for Oromia Regional Road Construction bureau and related private sectors use for future road construction planning to mitigate hazards of fissures.

1.9 Thesis Structure

This thesis has five chapters, each dealing with a particular topic of the research work. In this regard, Chapter 1 gives the general introduction, statement of the problem, objectives; significances of the study, methodology, previous work and structure of the thesis are presented. Chapter 2 generally deals with the regional geology, local geology and hydrogeology of the study area. Chapter 3 deliberates on the basic theoretical overview of geophysical techniques employed for this work. The 4^{th} Chapter presents geophysical data acquisition and processing procedures. Chapter five gives interpretations and discussion of results, conclusion and recommendations.

CHAPTER TWO

GEOLOGY, STRUCTURES AND HYDROGEOLOGY

2.1 Regional Geology

The Main Ethiopian Rift (MER) is a roughly NE-oriented segment of the East African Rift system, which extends from the Afar to the Kenya rift. The Ethiopian Rift extends for about 1000km in a NE–SW to N–S direction from the Afar depression, at the Red Sea–Gulf of Aden junction, southwards to the Turkana depression.

It has commonly been suggested that rift propagation in the MER progressed north wards (Wolfenden et al., 2004; Maguire et al.,2006; Keir et al.,2006), although its evolution is not well under stood. An alternative hypothesis implies south ward propagation. Bonini et al. (2005) suggested a heterogeneous time space evolution, with initial extension in the Southern MER at 20–21 Ma, followed by extension in the Northern MER at ~11Ma and finally formation of the Central MER at about 5–6Ma. Irregular rift propagation due to the presence of preexisting structures has also been proposed by (Keranen and Klemperer, 2007).

Tertiary to Quaternary volcanic are the only rocks exposed in the MER, apart from minor fluvio-lacustrine sediments, mostly of Quaternary age, that were deposited on the rift floor. One exception is an outcrop of Precambrian crystalline rocks covered by Mesozoic sediments at the base of the Guraghe escarpment, near the village of Kella about 80km south-west of Addis Ababa. Apart from Kella, basement rocks in the MER are exposed only in its extreme south and in the northern Afar (Tsegaye Abebe et al., 2010).

Volcanism started during the Eocene-late Oligocene with the eruption of flood basalts that have generally been related to either one or two mantle plumes impinging the base of the lithosphere under Afar or Afar-Northern Kenya rifts (Kim et al., 2012). The oldest flood basalts crop out in the broadly rifted zone of southern Ethiopia and are of Eocene in age (45Ma). Flood basalts forming the Ethiopian Plateau instead apparently erupted in a rather short time interval (<5Ma) with the greatest eruption rates occurring from 31 to 28Ma. From these early episodes of volcanism, magmatic activity in the MER was episodic rather than continuous. A second episode

of flood basalt volcanism has been described in the southern Ethiopia at 18-11Ma and in the MER-Afar transition zone at about 10–11Ma also been (Corti, 2009).

In the Central MER, early eruption of flood basalts was locally followed by under-saturated intermediate and acidic rocks (at 17–12Ma and by eruption of late Miocene (11–8Ma) basalts and subordinate silicic flows. After these episodes of pre rift activity (with wide spread flood basalts and subordinate felsic products), rifting in the various MER sectors was characterized by volcanism with fundamentally bi-modal character. Widespread late Miocene-Pliocene rhyolitic ignimbrites (7–3Ma) with intercalated minor mafic lavas occur throughout the Northern and Central MER. Mainly basaltic central volcanoes grew mostly on the Somalian plateau during Pliocene times, giving rise to an important phase of off-axis volcanism (Corti, 2009)

In the Quaternary (<1.6–1.8Ma), bimodal volcanic rocks (lava, pyroclastic and volcano clastic strata) were generally closely associated with Wonji Fault Belt affecting the rift floor. In the Southern MER, volcanic activity was resumed in the early Pleistocene with eruption of ignimbrites and basalts (Bonini et al., 2005).

2.2 Tectonic Setting and Structures

The Main Ethiopian Rift is bounded by discontinuous boundary faults that give rise to major fault escarpments separating the rift depression from the Ethiopian and Somalian plateaus. These faults are normally long, widely spaced and characterized by large vertical offsets (>1km; e.g., Boccaletti et al., 1998). Their orientation varies in the different rift segments.

Active faulting and volcanic activity is mostly localized along an N-S to N20 trending fault system (Wonji Fault Belt) developed within the rift floor.

The Northern MER is considered to extend from the true Afar depression up to the Lake Koka region following the middle course of the Awash River valley. The main boundary faults in this region show an average N50 trend and formed since about 10–11 Ma. Early synrift volcanism in the area started at about 10–11 Ma (Keranen and Klemperer, 2007).

The Central MER encompasses most of the Lakes Region, up to the Lake Awassa area (Figure 2.1). Here, the main boundary faults trend roughly N30–35 and the age of faulting onset is estimated to be around 8.3–9.7 Ma, while the age of the earliest synrift volcanic deposits is suggested to be 8 Ma.

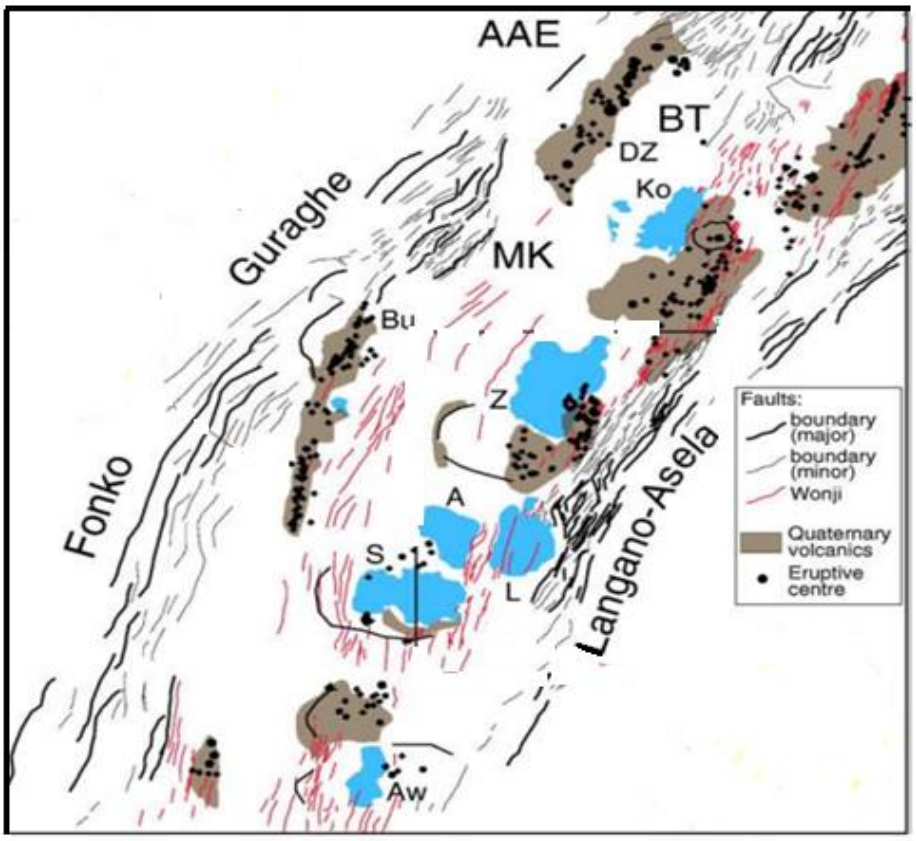

Figure 2.1. Structural setting of the Central MER (A: Lake Abiyata; Aw: Lake Awassa; L: Lake Langano; S: Lake Shala; Z: Lake Ziway and Bu: Butajira volcanic chain (adopted from Corti, 2009).

The Southern MER extends south of Lake Awassa into the 300-km-wide system of basins and ranges (referred to as broadly rifted zone) that characterizes the overlapping area between the Ethiopian and Kenya Rifts. Faults in the Southern MER show a dominant N-S to N20 trend and were well established after 18 Ma, whereas volcanism started in the early Miocene around 18–21 Ma.

These three segments represent different stages of the extension process, from early rifting in the Southern MER to more evolutionary stages in the Central and Northern MER preceding the incipient seafloor spreading in Afar. However, the age of onset of faulting and volcanism outlined above for the three rift segments point to a heterogeneous time-space evolution and progression of the continental rifting process along the MER (Keranen and Klemperer, 2007).

2.3 Local Geology and Hydrogeology of Study Area

The study area is covered by the geologic units like ignimbrites, tuff and local basalts. Figure 2.2 gives the geological as well as the hydrogeological map of the study are and its surroundings. The hydraulic conductivity of geologic units is low (Shemelis Fikre, 2006). In the area, there is no surface water and the peoples in the area have the problem of water.

2.4 Well Log Data

Two wells are available in the close proximity of the study area. The two wells are located at Awasho Danku that is on the eastward side of Shashamane and drilled by Atlas water Well Drilling PLC. The two well geologic descriptions and their depths are described in the Tables 2.1 and 2.2. The well location of Table 2.1 is about 3km from Shashamane town with specific location of 794550N and 460393E at an altitude of 1919amsl. This well was drilled in 2014 to a depth of about 286m. The lithological description of the second well in close proximity to the fissured area is given in Table 2.2. This well is about 7km from Shashamane with specific location of 795210N and 462737E at an altitude of 2098amsl. The depth of this well is about 400m.

Table 1. Well log data (Awasho Danku, Well 1)

No	Depth Range(m)	Geological descriptions
1	0-1	Black top Clay soil
2	1-30	Tuff
3	30-40	Tuff with Clay
4	40-50	Highly weathered Ignimbrite
5	50-60	Moderately weathered Ignimbrite
6	60-80	Moderately weathered and fractured Ignimbrite
7	80-90	Tuff

8	90-110	Ignimbrite
9	110-120	Slightly weathered and fractured Ignimbrite
10	120-140	Paleosoil
11	140-160	Highly weathered and fractured Ignimbrite
12	160-180	Fractured Basalt with Sand
13	180-200	Slightly weathered and fractured Ignimbrite
14	200-210	Paleosoil
15	210-250	Pumice with Sand
16	250-286	Massive Basalt

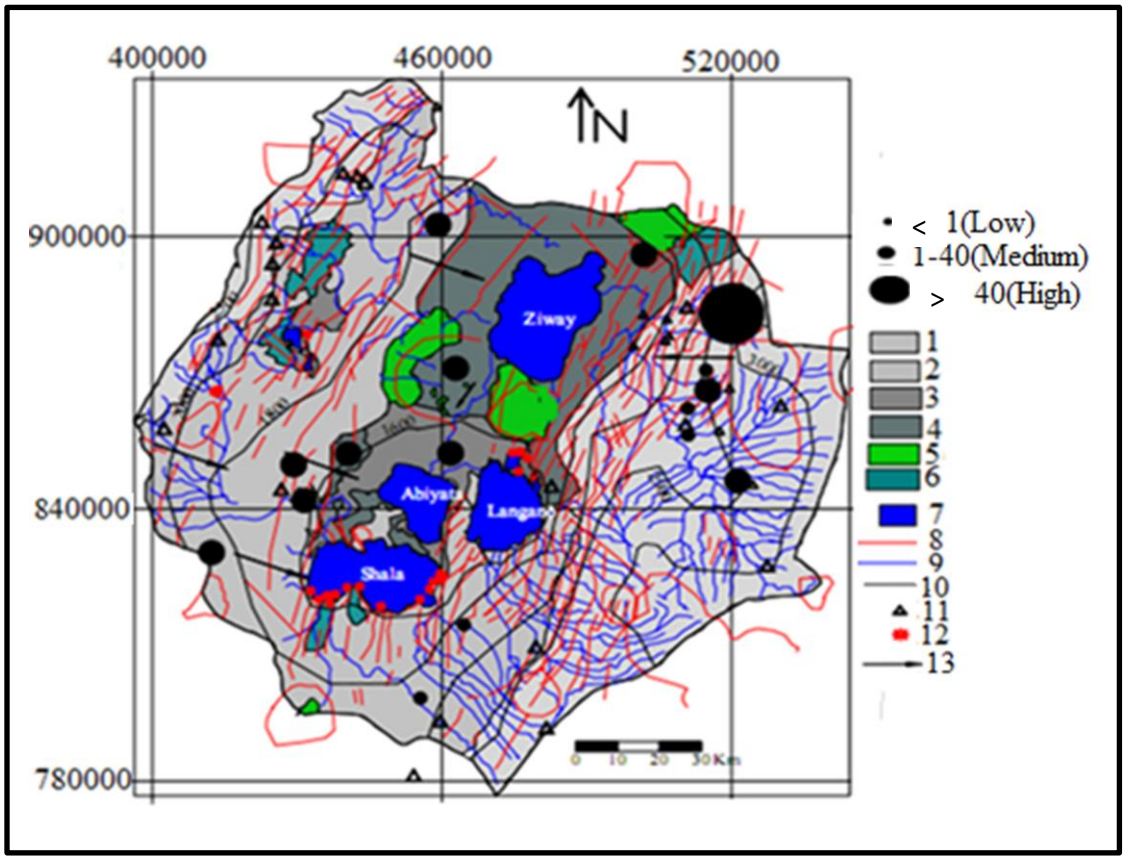

Figure 2.2.Geological and Hydrogeological map of the study area and its surroundings (1- Ignimbrite, tuff, local rhyolite, 2- Ignimbrite, tuff, local basalt, 3- Ignimbrite covered with lacustrine soils, recent regression, 4- Ignimbrite covered with lacustrine deposit, 5- Rift volcanoes and volcanic ridges, 6-Basalt, local ignimbrite,7- Lake, 8- Volcano tectonic structures, 9- Drainage, 10-Groundwater level contour, 11-Cold spring, 12- Hot spring, 13-Groundwater flow direction, circles represent the hydraulic conductivity (after Shemelis Fikre, 2006).

Table 2. Well log data (Awasho Danku, Well 2)

No	Depth range(m)	Geological descriptions
1	0-1	Sandy soil
2	1-2	Very fine and very sorted Pumice
3	2-13	Slightly weathered and fractured Tuff
4	13-16	Highly weathered and fracture Scoriaceous Basalt
5	16-20	Very fine Sand
6	20-63	Unwelded tuff
7	63-67	Tuff
8	67-71	Rock fragment
9	71-176	Highly weathred and fractured Ignimbrite
10	176-198	Scoriaceous Basalt
11	198-215	Slightly weathered Ignimbrite
12	215-395	Moderately weathered and fractured Ignimbrite
13	395-400	Highly weathered and fractured Ignimbrite

CHAPTER THREE

GEOPHYSICAL METHODS

3.1 General

The science of geophysics applies the principles of physics to the study of the Earth. Geophysical investigations of the interior of the Earth involve taking measurements at or near the Earth's surface that are influenced by the internal distribution of physical properties. Analysis of these measurements can reveal how the physical properties of the Earth's interior vary vertically and laterally. An alternative method of investigating subsurface geology is, of course, by drilling boreholes, but these are expensive and provide information only at discrete locations.

There is a broad division of geophysical surveying methods into those that make use of natural fields of the Earth and those that require the input into the ground of artificially generated energy. The natural field methods utilize the gravitational, magnetic, electrical and electromagnetic fields of the Earth, searching for local perturbations in these naturally occurring fields that may be caused by concealed geological features of economic or other interest. Artificial source methods involve the generation of local electrical or electromagnetic fields that may be used analogously to natural fields, or, in the most important single group of geophysical surveying methods, the generation of seismic waves whose propagation velocities and transmission paths through the subsurface are mapped to provide information on the distribution of geological boundaries at depth.

Generally, natural field methods (passive methods) can provide information on earth properties to greater depths and are simpler to carry out than artificial source methods (active methods). Moreover, the artificial source methods are capable of producing a more detailed and better resolved picture of the subsurface geology.

It is the local variation in a measured parameter, relative to some normal background variation is attributed to a localized subsurface zone of distinctive physical property and possible geological importance. A local variation of this type is known as a geophysical anomaly.

3.2 The Electrical Resistivity Method

There are many methods of electrical surveying. Some make use of fields within the Earth while others require the introduction of artificially-generated currents into the ground.

In the resistivity method, artificially-generated electric currents are introduced into the ground and the resulting potential differences are measured at the surface.

The resistivity method is used in the study of horizontal and vertical discontinuities of the ground. It can also be used in the detection of three-dimensional bodies of anomalous electrical conductivity. It is routinely used in engineering and hydrogeological investigations of shallow subsurface geology. The method uses artificially-generated low frequency electric currents, introduced into the ground and the resulting potential differences are measured at the surface.

3.2.1 The resistivity of Earth materials

The resistivity of geological materials exhibits one of the largest ranges of all physical properties, from $1.6 \times 10^{-8}\Omega$ m for native silver to 10^{16} Ωm for pure sulphur. Igneous rocks tend to have the highest resistivity; sedimentary rocks tend to be most conductive, largely due to their high pore fluid content; and metamorphic rocks have intermediate but overlapping resistivity. The age of a rock also is an important consideration: a Quaternary volcanic rock may have a resistivity in the range 10-200 Ωm while that of an equivalent rock but Precambrian in age may be an order of magnitude greater. This is a consequence of the older rock having far longer to be exposed to secondary infilling of interstices by mineralization, compaction decreasing the porosity and permeability, etc. (Reynolds, 1997).

The ability of a medium to conduct an electric current is termed electrical conductivity σ (S/m) and the inverse of it is called electrical resistivity ρ (Ωm). Or Resistivity = 1 / Conductivity

Resistivity surveying investigates variations of electrical resistance, by causing an electrical current to flow through the subsurface using wires (electrodes) connected to the ground.

3.2.2 Apparent resistivity

By measuring ΔV, I and knowing the Electrode configuration, we obtain a resistivity ρ. If the ground is homogenous, the potential difference measured is as a function of the true resistivity of the homogeneous earth and the geometric factor (Telford et al., 1990). But in reality the ground is locally in the homogeneous and the potential difference depends on the current applied, the resistivity of the sub surface medium and the geometrical factor (K) determined by electrode array or configurations types. The resistivity calculated from such non homogenous ground is not a true resistivity rather it is called apparent resistivity (ρ_a).

The apparent resistivity is the value obtained as the product of a measured resistance (R) and a geometric factor (K) for a given electrode array, according to the (equation 3.1). The geometric factor takes into account the geometric spread of electrodes and contributes a term that has the unit of length (meters). Apparent resistivity (ρ_a) thus has units of ohm-meters and expressed as.

$$\rho_a = K\frac{\Delta V}{I} \qquad (3.1)$$

where $\rho_a = RK$ and $R = \Delta V/I$

For this study, Schlumberger array is used. Apparent resistivity for Schlumberger array is given as:

$$\rho_a = \pi\frac{a^2}{b}\left[1-\frac{b^2}{4a^2}\right]R; a \geq 5b \qquad (3.2)$$

where the quantity

$$K = \pi\frac{a^2}{b}\left[1-\frac{b^2}{4a^2}\right]$$

is called the geometric factor of the array.

The apparent resistivity has to be interpreted using curve matching or inversion techniques to find estimated resistivity versus depth of the subsurface.

3.2.3 Resistivity sounding principles

For this study VES is typically carried out in Schlumberger array, where the potential electrodes are placed in a fixed position with a short separation and the current electrodes are placed symmetrically on the outer sides of the potential electrodes. After each resistivity measurement the current electrodes are moved further away from the center of the array. In this way the current is stepwise made to flow through deeper and deeper parts of the ground. For large distances between the current electrodes, the distance of the potential electrodes is increased to ensure that the measured voltage is above the noise level and the detection level in the instrument.

For a VES in Schlumberger array, the distance between the current electrodes should be about 250 m to detect a resistivity layer boundary in the depth of 50 m. The penetration depth depends on the chosen electrode array, maximum electrode spacing and the data density.

3.2.4 Dipole-Dipole arrays

The Dipole-Dipole array is logistically the most convenient in the field, especially for large spacing. All the other arrays require significant lengths of wire to connect the power supply and voltmeter to their respective electrodes and these wires must be moved for every change in spacing as the array is either expanded for a sounding or moved along a line. The convention for the Dipole-Dipole array shown below in Figure 3.1 is that current and voltage spacing is the same, a, and the spacing between them is an integer multiple of a.

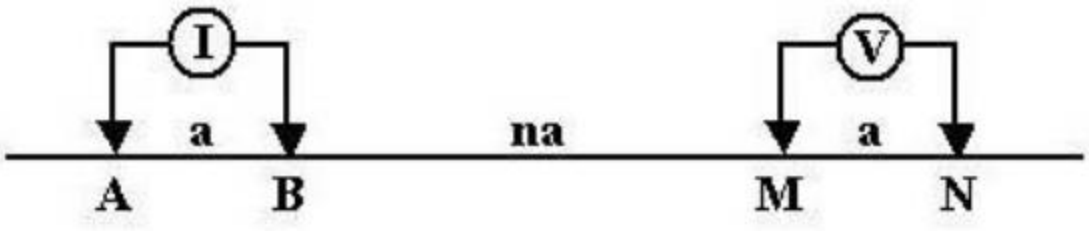

Figure 3.1.The Axial Dipole-Dipole arrangement.

The apparent resistivity is given by:

$$\rho_a = \frac{V}{I}\pi an(n+1)(n+2) \tag{3.3}$$

Dipole-Dipole arrays are normally used in profiling mode to map lateral as well as depth variations in resistivity. The plotting convention is to plot the values of apparent resistivity (equation 3.3) at the intersection point of two 45˚ lines descending from the current dipole and from the potential dipole. The resulting "maps" of apparent resistivity are contoured at constant (usually logarithmic) intervals. The contoured sections are called "pseudo sections" because they look somewhat like resistivity cross-sections of the ground but they are not, they are simply a graphical representation of the data. The vertical scale is not depth but some function of the array spacing. For some geological models the pseudo sections do have an intuitive relationship to the actual section but mostly they do not. For a layered earth the contours are horizontal and rise and fall in value in the same sense as the actual resistivity, but for the case of a vertical contact between dissimilar resistivity's the pseudo-section is a complex map with no direct relationship to the actual model.

3.3 Magnetic method

3.3.1 Principles and elementary theory

If two magnetic poles of strength p_1 and p_2 are separated by a distance r, a force exists between them is given by:

$$F = \frac{p_1 p_2}{4\pi\mu r^2} \tag{3.4}$$

where μ is the magnetic permeability of the medium separating the poles; p_1 and p_2 are pole strengths and r the distance between them. The force is attractive if the poles are different in sign and repulsive if they are of like sign.

3.3.2 The Earth's Magnetic Field

The geomagnetic field at or near the surface of the earth originates largely from within and around the earth's core. Magnetic anomalies caused by rocks are localized effects superimposed on the normal magnetic field of the Earth (geomagnetic field).

The total field vector B has a vertical component Z and a horizontal component H in the direction of magnetic north. The dip of B is the inclination I of the field and the horizontal angle between geographic and magnetic north is the declination D. B varies in strength from about 25000nT in equatorial regions to about 70000nT at the poles (Kearey et al., 2002).

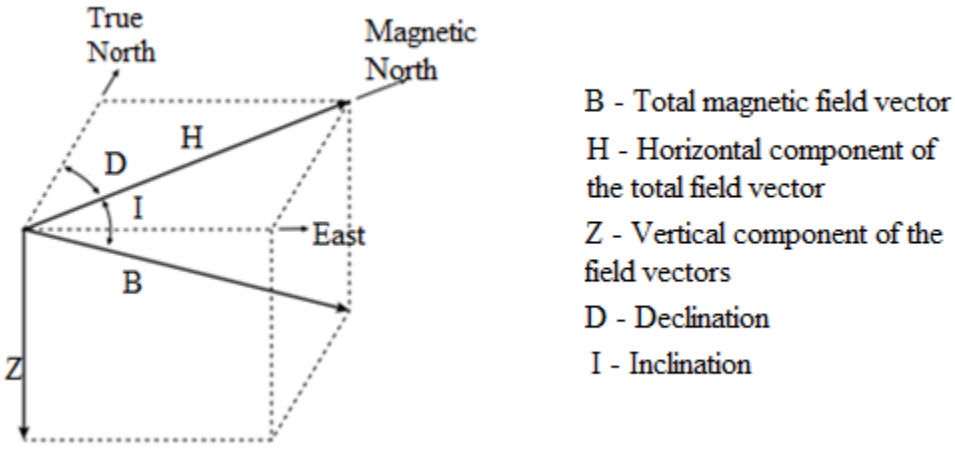

Figure 3.2.The elements of the geomagnetic field.

where, $B^2 = H^2+Z^2$, $I = \tan^{-1}(Z/H)$, $D = \tan^{-1}(H_E/H)$ with H_E –East component of horizontal field vector.

In general, there are three components of the Earth's magnetic field.

- **The main field or dipole field (B_D)**, this is produced in the fluid outer core of the earth and accounts for the very large regional variations in the total field intensity and direction.

- **The external magnetic field (B_{ext}),** is a relatively small portion of the observed magnetic field that is generated from magnetic sources external to the earth. This is produced by electric currents in the earth's atmosphere consisting of particles ionized by solar radiation and put into motion by solar tidal force.
- **The crustal or anomalous magnetic field (B_{rm}),** this is the portion of the magnetic field associated with the magnetism of crustal rocks. This portion of the field contains magnetism caused by induction from the Earth's main magnetic field and from remnant magnetization.

The earth's total magnetic field B_T is thus given as:

$$B_T = B_D + B_{ext} + B_{rm} \tag{3.5}$$

where B_T is the total magnetic field, B_{ext} is external magnetic field and B_{rm} is rock magnetic field, with B_{ext} =0.1˚ of B_T: B_D =99˚ of B_T: rock magnetism B_{rm} is variable and the weakest of B_{ext} and B_D.

3.3.3 Temporal variation of the earth's magnetic field.

It is variation of the Earth's magnetic field with time. Temporal variations of the Earth's magnetic field are classified into three types depending on their rate of occurrence and source.

- **Diurnal variations**: These are variations in the magnetic field that occur over the course of a day and are related to variations in the Earth's external magnetic field. This variation can on the order of $20 - 30\gamma$ per day and should be accounted for when conducting exploration magnetic surveys.
- **Magnetic storms:** Occasionally, magnetic activity in the ionosphere will abruptly increase. The occurrence of such storms correlates with enhanced sunspot activity. The magnetic field observed during such times is highly irregular and unpredictable, having amplitudes as large as 1000γ. Exploration magnetic surveys should not be conducted during times of magnetic storms. This is simply because it is difficult to correct for magnetic storms in the acquired data.

- **Secular variations:** these are long-term (changes in the field that occur over years) variations in the main magnetic field that are presumably caused by fluid motion in the Earth's outer core. Since these variations occur slowly with respect to the time of completion of a typical exploration magnetic survey, secular variations will not complicate data reduction efforts of the acquired field data.

3.3.4 Magnetic surveying

The surveying of magnetic anomalies can be carried out on land, at sea and in the air. In a simple land survey an operator might use a portable magnetometer to measure the field at the surface of the Earth at selected points.

The purpose of magnetic surveying is to identify and describe regions of the Earth's crust that have unusual (anomalous) magnetizations. In the realm of applied geophysics the anomalous magnetizations might be associated with local mineralization that is potentially of commercial interest, or they could be due to subsurface structures.

Ground magnetic surveys are usually performed over relatively small areas on a previously defined target. Consequently, station spacing is commonly of the order of 10–100m, although smaller spacing may be employed where magnetic gradients are high. Readings should not be taken in the vicinity of metallic objects such as railway lines, cars, roads, fencing, houses, etc., which might perturb the local magnetic field. For similar reasons, operators of magnetometers should not carry metallic objects.

Base station readings are not necessary for monitoring instrumental drift as fluxgate and proton magnetometers do not drift, but are important in monitoring diurnal variations.

Since modern magnetic instruments require no precise leveling, a magnetic survey on land invariably proceeds much more rapidly than a gravity survey.

3.3.5 Magnetic data reduction

The reduction of magnetic data is necessary to remove all causes of magnetic variation from the observations other than those arising from the magnetic effects of the subsurface geology. These reductions are:

Diurnal variation correction:

It is correction applied to the variation in intensity of the geomagnetic field at the Earth's surface during the course of a day. This diurnal variation is due to the part of the Earth's magnetic field that originates in the ionosphere. The diurnal variation is corrected by installing a constantly recording magnetometer at a fixed base station within the survey area. The time is noted at which each field measurement is made during the actual survey. The differences observed in base readings are then distributed among the readings at stations occupied during the day according to the time of observation. Base readings are taken solely to correct for temporal variation in the measured field.

Diurnal variations, however recorded, must be examined carefully. If large, high-frequency variations are apparent, resulting from a magnetic storm, the survey results should be discarded.

Geomagnetic correction

In order to produce a magnetic anomaly map of a region, the data have to be corrected to take in to account the effect of latitude and to a lesser extent longitude. As the Earth's magnetic field strength varies from 25000nT at the magnetic equator to 70000nT at the poles, the increase in magnitude with latitude needs to be taken in to account (Reynolds, 1997). Survey data at any given location can be corrected by subtracting the theoretical field value B_{th}, obtained from the international geomagnetic reference field (IGRF) from the measured value, B_{obs} as equitation 3.6. Therefore, the magnetic anomaly (ΔB), obtained by subtracting the diurnal correction (δB_D) and geomagnetic correction (B_{th}) is given by:

$$\Delta B = B_T - \delta B_D - B_{th} \tag{3.6}$$

An alternative method of removing the regional gradient over a relatively small survey area is by use of trend analysis. A trend line (for profile data) or trend surface (for areal data) is fitted to the observations using the least squares criterion, and subsequently subtracted from the observed data to leave the local anomalies as positive and negative residuals.

CHAPTER FOUR

DATA ACQUISITION AND PROCESSING

4.1 General

The choice of geophysical techniques for subsurface investigation depends on the objectives of the problem to be solved. All geophysical methods are not equal in solving a particular problem, some are better than the others. The other factor that constrains the choice of geophysical methods are availability of instrument, field conditions (space, artificial noise) etc. Based on these factors that constrain the methods it has been decided that the methods to be used in the current work are electrical resistivity (VES and Dipole-Dipole) and magnetic methods.

4.2 Electrical Resistivity Survey

4.2.1 Instruments used and field procedure

The instrument used for electrical resistivity sounding and Dipole-Dipole resistivity profiling survey is IRIS Syscal R1 plus Switch 72 system. The Schlumberger electrode configuration was used for vertical electrical sounding measurement with maximum half-current electrode separation (AB/2) of about 500m. The current electrode separation distance progressively increase and with large current electrode distance potential electrode separation also increased due to the fact that with increase in current separation distance the value of potential difference decrease. In each case, the sounding curve, which is a log-log graph of apparent resistivity versus AB/2, was plotted, right in the field as a measure quality control. If any error is detected during data acquisition, it was automatically corrected either by taking repeated measurements, by improving the ground contact resistance of the electrodes or by changing the position of the measuring electrodes.

Dipole-Dipole profiling was used for lateral inhomogeneity hunting of subsurface. The configuration used is axial Dipole-Dipole configuration. It is achieved by keeping the separation between the electrodes fixed (to the depth required by the survey) with an electrode spacing of 10m and moving the two electrodes (current or potential two) up to the six slices depth and fixe

the other two electrodes, then after the rest two electrode moves to the next place and two electrodes moves to six slice depth and the procedure continue until the required distance achieved on the surface along the selected profile/survey line.

4.2.2 Data acquisition and processing

A total of three VES soundings were made using Schlumberger field array along one profile as in Figure 4.3. The station spacing between VES-1 and VES-2 is about 284m while that between VES-2 and VES-3 is about 619m, i.e. the total distance from VES-1 to VES-3 is about 903m. All the VES arrays are oriented approximately in the E-W direction. In all cases the sounding curves have segmented overlapped measurement points at a distance of AB/2 = 20, 30, 150, and 220m with different potential distance of MN = 1.5, 6 and 45m. And is impossible for segments to cross each other and they cannot be interpreted as it is but the win resist software average out the overlapping point values and gives as one interpretable curve. A typical sounding curve interpreted using the Win Resist software is as given in Figure 4.1.

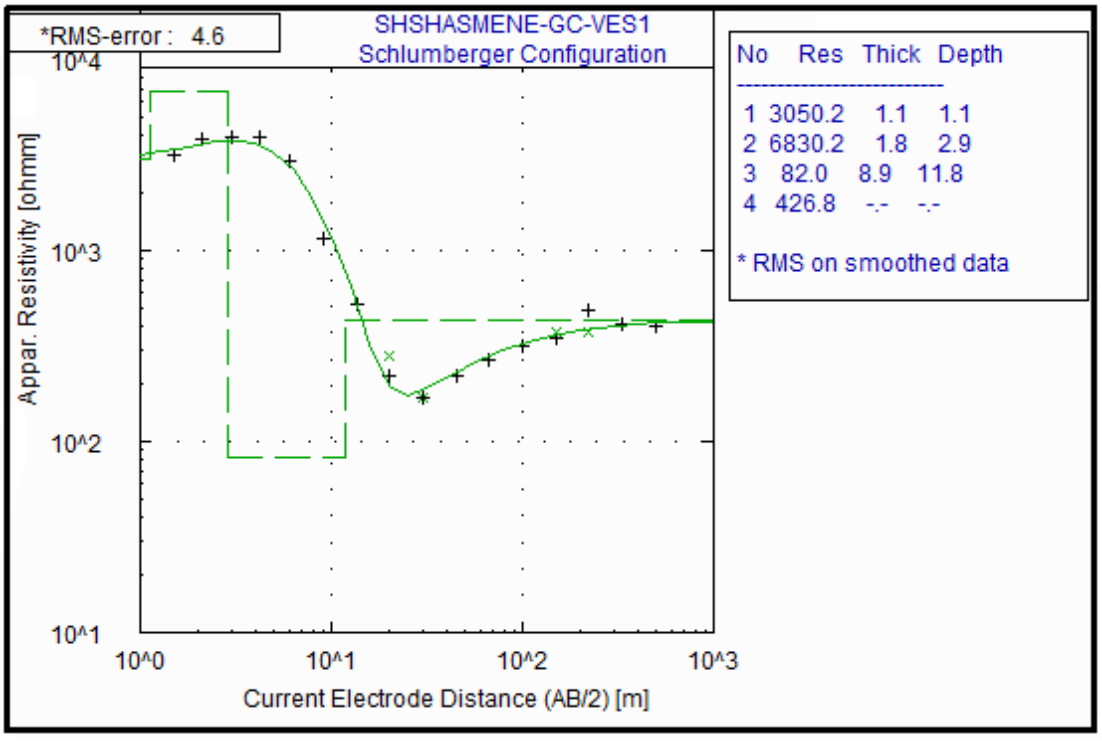

Figure 4.1. Interpreted sounding curve for VES-1, Oine Chafo Umbure ground fissure, Shashamane.

On the other hand, a total of about 276 point data was collected along the two selected axial Dipole-Dipole profiling lines with an electrode spacing of 10m over 6 slice depths as shown in Figure 4.3 with DP1 (Dipole Profile 1) and DP2(Dipole profile 2). The length of the first line is about 280m and that of the second line is about 210m.The data was processed by using RES2DINV Inversion software and a typical interpreted section of the profile 1 is shown in Figure 4.2. This program automatically subdivide the subsurface into a number of blocks and then uses a least-squares inversion scheme to determine the appropriate resistivity values for each blocks so that the calculated apparent resistivity values agrees with the measured apparent resistivity values from the field survey. The quality of fit is called route mean square error (RMS) and expressed in percent. The results are displayed as inverted model resistivity sections versus depth of the subsurface along each profile.

4.3 Magnetic Surveys

4.3.1 Instruments used and field procedure

The instrument used in magnetic survey was Proton Precision Magnetometer which measures total magnetic field intensity. The survey was conducted with a single Proton Precision Magnetometer for survey used both as base station and field magnetometer. Before any measurement was taken, two base stations were established. The first base station (B1 in Figure 4.3) was established at coordinates (450933E, 798538N) and used while carrying out surveys on the first three profiles (P1 to P3, Figure 4.3). While the survey for the remaining 3 profiles (P4 to P6, Figure 4.3) was conducted using the base station (B2 in Figure 4.3) located at (450699E, 798328N). Base station readings were taken at the starting and end of each survey line which is with a time gap of about 30 minutes. Readings at field station over all the survey lines and at the base station were taken three times and the average values were recorded.

4.3.2 Data acquisition and processing

The magnetic data were collected perpendicular to the strike of the cracks along six selected lines in the study area oriented approximately North-west to South-east in direction (Figure 4.3). In this study a total of about 141 magnetic data has been collected. The field observed magnetic data were corrected for diurnal variation using the base station reading taken at the beginning

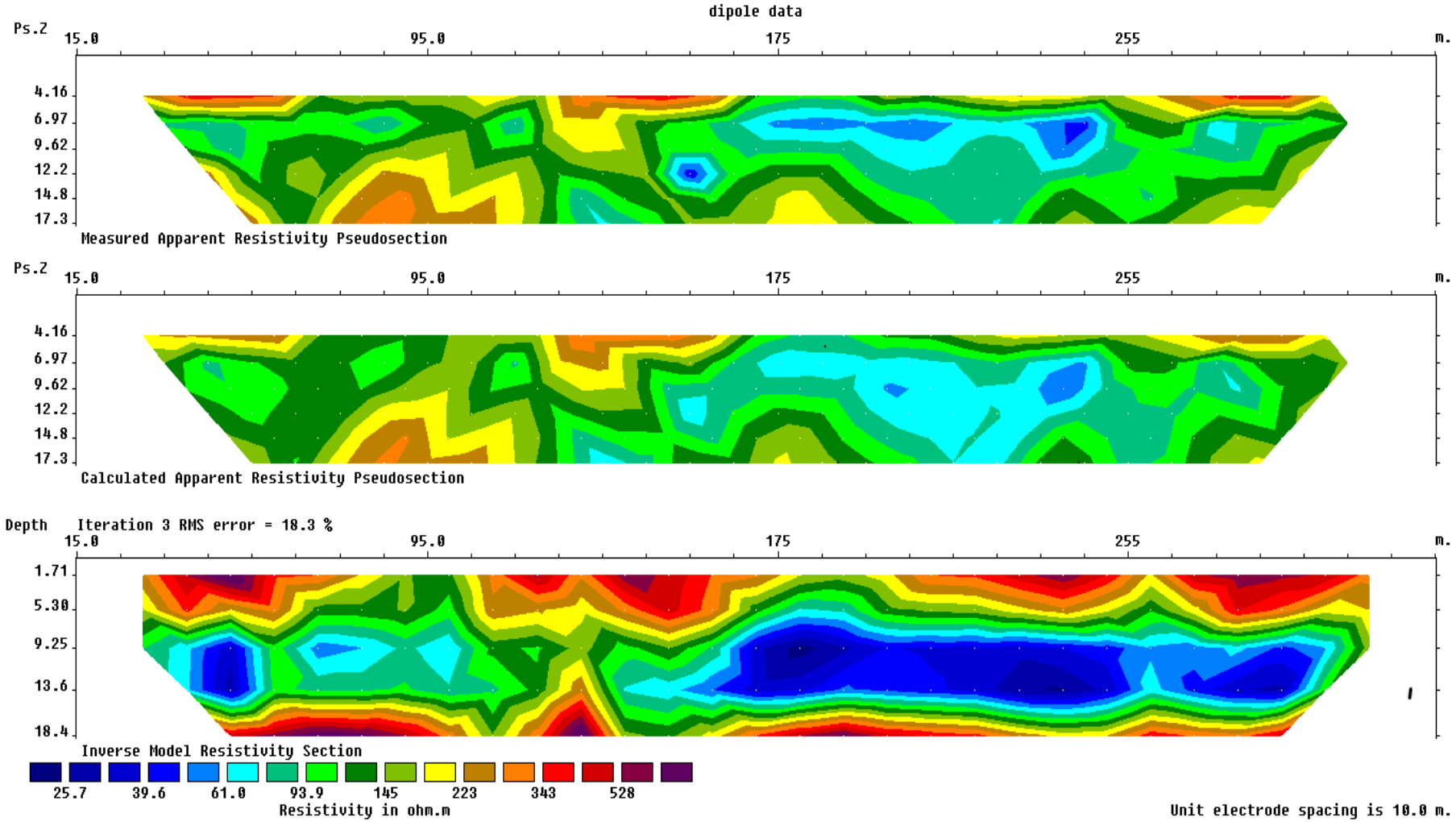

Figure 4.2. Measured, calculated apparent resistivity pseudosections and inverse model resistivity section plot for Profile-1, Oine Chafo Umbure ground fissures, Shashamane.

and end of each survey line. Then after drift correction, International Geomagnetic Reference Field (IGRF) corrections have been done by subtracting theoretical magnetic field value.

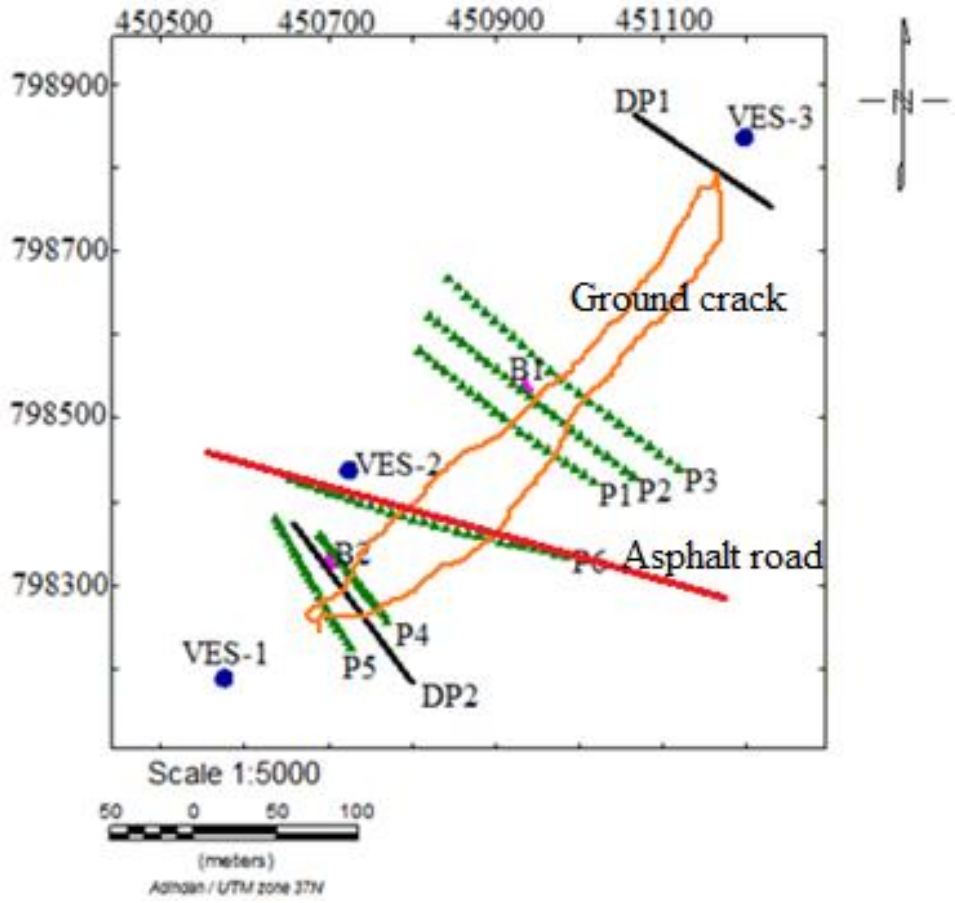

Figure 4.3. The geophysical survey traverses, Oine Chafo Umbure ground fissure, Shashamane.

4.3.2.1 Magnetic data reduction

To remove all causes of magnetic variation from the observations other than those arising from subsurface geology it is necessary to make a correction to magnetic raw data. Therefore, all the primary magnetic data collected were corrected for diurnal effects and for the variations caused by dipole field. Diurnal correction for each magnetic data was computed by using the formula:

$$\delta B_D = \gamma i \pm (\Delta\gamma / \Delta T)(T_s - T_1) \qquad (4.1)$$

where δB_D - diurnal corrected data measured at time Ti , γi - magnetic field measured at time Ti , $\Delta\gamma = \gamma_2 - \gamma_1$, γ_1 - base station reading at the start of field survey and γ_2 - base station reading at the end of the survey, $\Delta T = T_2 - T_1$, T_1 - base station time reading at the beginning of the survey, T_2 - base station time reading at the end of the survey, T_s survey station reading time.

The geomagnetic correction is a technique that removes the effect of geomagnetic references field from the survey data. It is corrected by using the International Geomagnetic Reference Field (IGRF) value.

The total magnetic field anomaly was obtained after the removal of diurnal variation and IGRF correction. Finally the total magnetic intensity map, magnetic anomaly map, analytical signal map and 2D modeling are produced using Oasis Montaj software for effective interpretation of the obtaining magnetic data.

CHAPTER FIVE

INTERPRETATION AND DISCUSSION OF RESULT, CONCLUTION AND RECOMMENDATION

5.1 Interpretation and Discussion of Results

5.1.1 Resistivity survey

The VES resistivity data were presented interms of, apparent resistivity pseudo depth section, interpreted sounding curves and geoelectric section.

a. Apparent resistivity pseudo section

The apparent resistivity pseudo section along the selected line is mapped from raw data using surfer software as shown in figure 5.1 . The pseudodepth section is constructed for the 3 VES data that lie on the survey traverse Line.

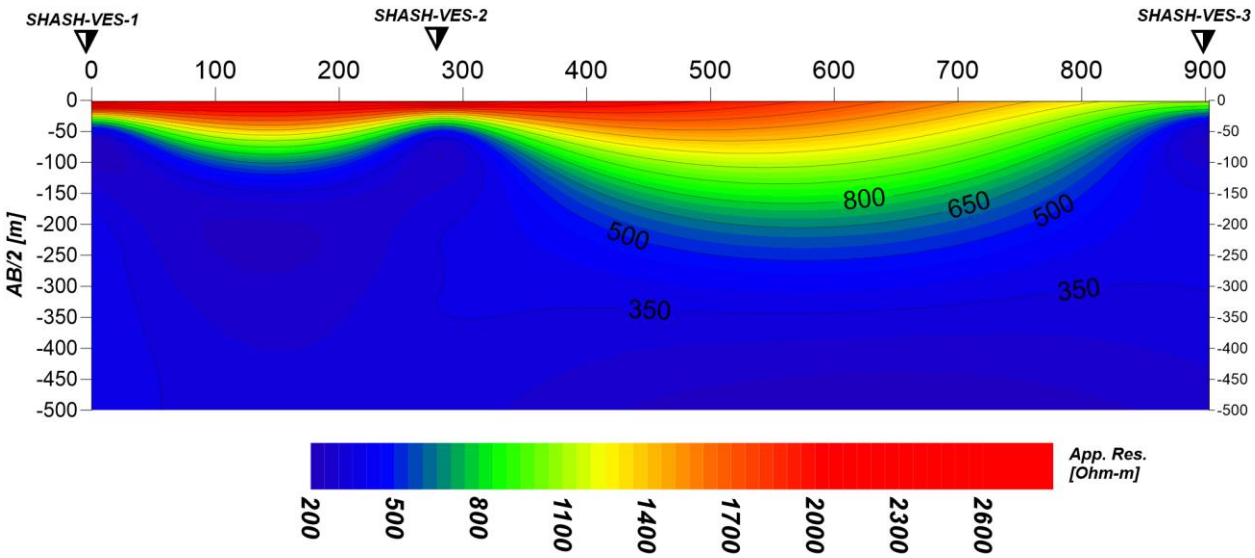

Figure 5.1. Apparent resistivity pseudo section along the VES Profile, Oine Chafo Umbure Ground fissure, Shashamane.

For the construction depth value used is negative of a half current electrode spacing (AB/2) and distance is spacing between VES points. According to the figure, shallow zones (approxmatily up to depth of 50m) have high resistivity and the rest larger part have low resistivity value (relative to the top) with resistivity decrease from top to bottom.

b. Interpreted Sounding Curves

The three sounding data were interpreted using the Winresist software to obtain the layer parameters (resistivity and tickness of the individual layers) mapped with the survey (Figure 5.2). Model layer parameters were introduced to the WinResist software using visual inspection of the sounding curves. All the three sounding curves are found to be well interpreted with an RMS error of 4.6 to 2.5. The curves have been interpreted interms of four layer Earth with varying thickness and resistivity.

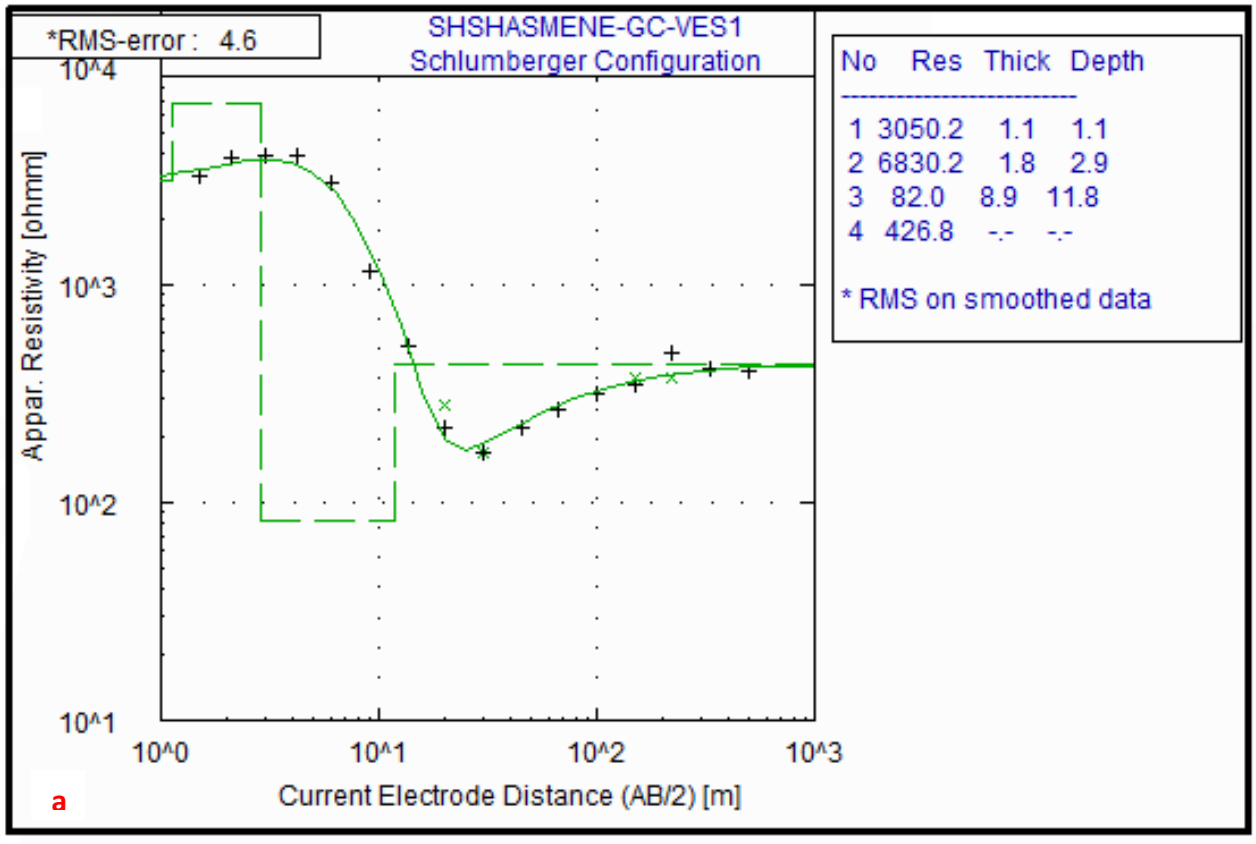

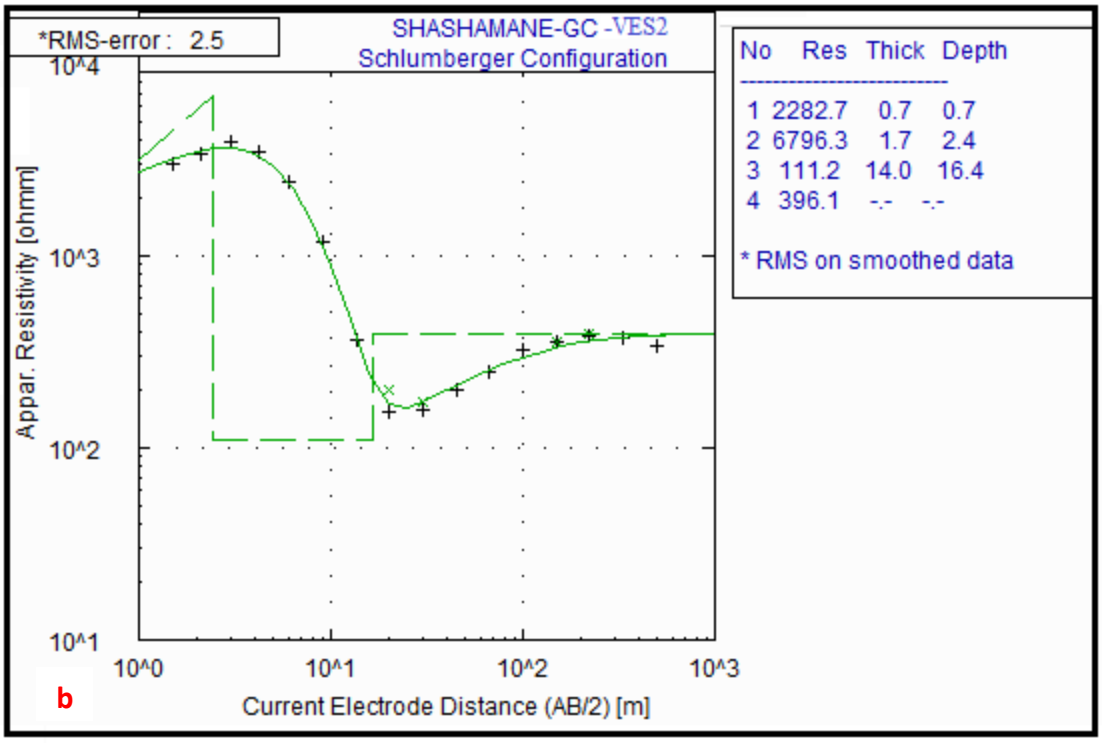

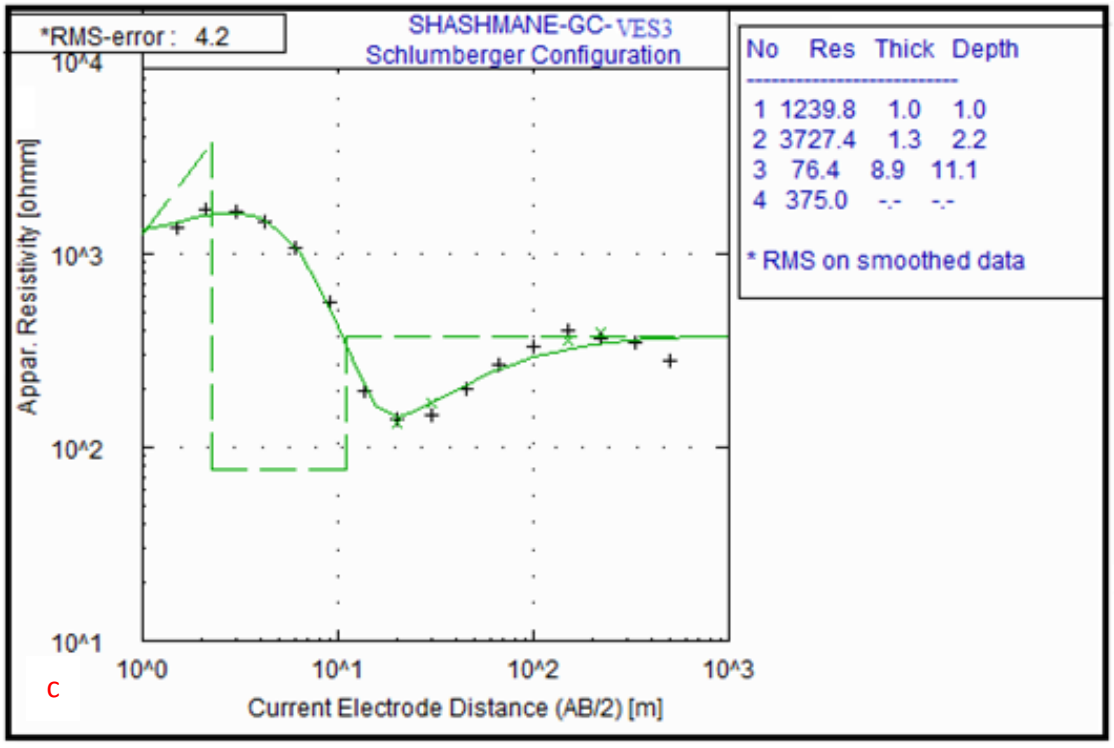

Figure 5.2. (a, b, c). Interpreted layer parameters of the three sounding data, Oine Chafo Umbure Ground fissure, Shashamane.

c. Geoelectric section

The resulting geoelectric section constructed from the interpreted layer parameters of the 3 VES laying on the traverse is given in Figure 5.3. A borehole located near survey area was also used to constrain depth and identify the lithological units beneath these VES points during modeling. In essence, the lithological description of the borehole depth section with their resistivity parameters from each interpreted VES were used to prepare the geoelectric section.

Geoelectric section along the selected line is constructed from the interpreted layer parameters of each VES points. In interpreting these field curves, WinResist software were used with optimal RMS error of about 4.6 to 2.5 which is acceptable value. The layer parameters (depth and apparent resistivity) were obtained using the software. These layer parameters were then used to construct the geoelectric section in AutoCAD 2007 software. The geology of geoelectric section was determined from well log data.

From the section given in Figure 5.3, it is seen that the subsurface consists of 4 geoelectric horizons. The layer representing the top part of the section (top soil), shows large variations of resistivity (1240 to 3050 Ohm-m) with thicknes of about 1m and are believed to be result of difference in soil moisture content in the soil.

Beneath these layers is a relatively high resistivity horizon (3727 to 6830 Ohm-m), with lithology of dry pumice. Its thickness extends from a depth of about 1m to 2.5m.

The third layer have resistivity range of (76 to 111 Ohm-m). Its lithologic unit is tuff and with thicknes of about 9m.The fourth layer have resistivity range of (375 to 427 Ohm-m). Its lithologic unit is weathered and fructured scoracious basalt at a depth below 12m.

d. 2D inverse model resistivity section.

The measured Dipole-Dipole resistivity profile data were processed using the RES2DINV software and the results are displayed as inverted model resistivity sections versus depth of the subsurface along each profile.

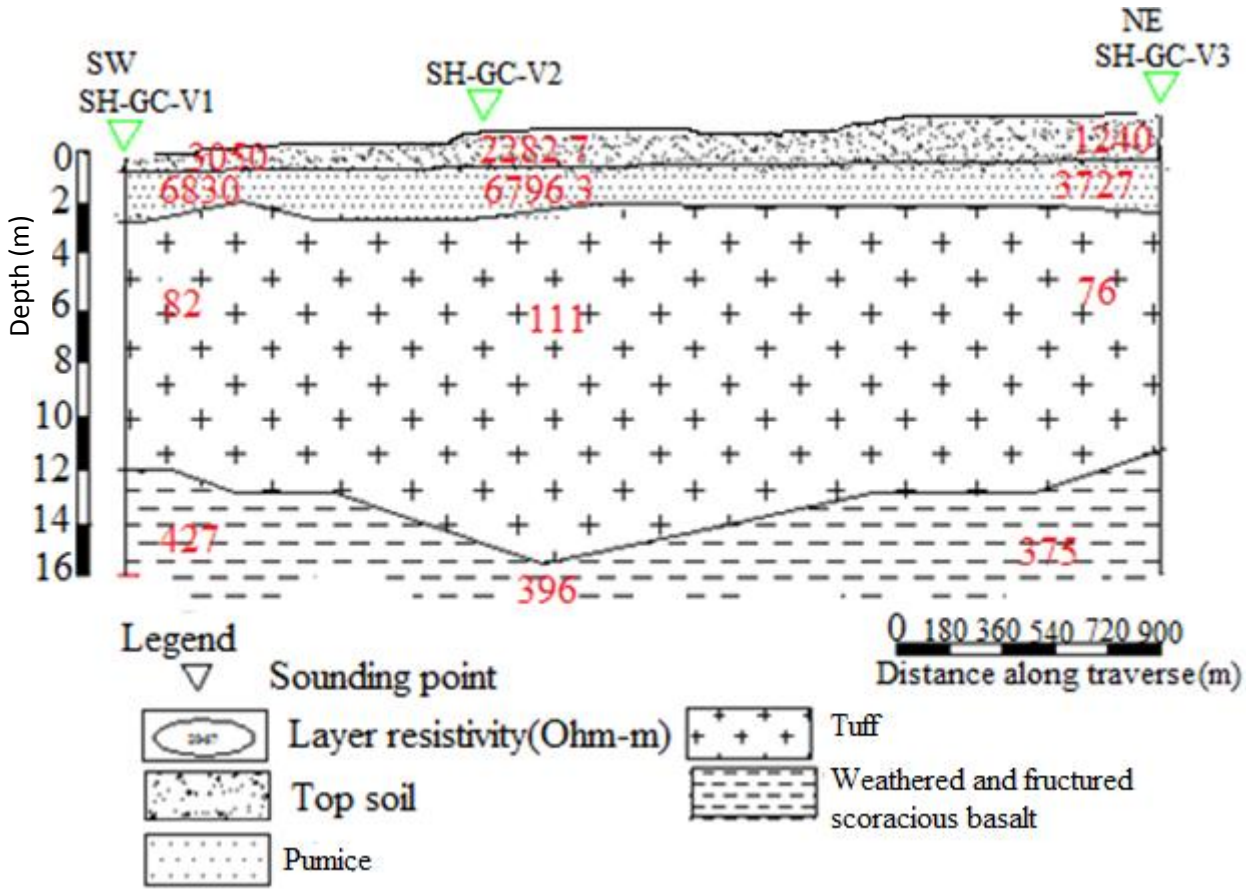

Figure 5.3. Geoelectric section along the sounding survey traverse, Oine Chafo Umbure, Shashamane.

I. Dipole-Dipole resistivity inverse model section for Profile-1

The 2D inverse model section of the Profile-1 (Figure 5.4) shows that the subsurface of first layer on the basis of resistivity variations is characterized by a zone of high resistivity between 100 to 530 Ohm-m with some discontinuity at a distance 95m and 185m and its overall thickens is 6m and which is interpreted in terms of lithological unit as a dry pumice and its resistivity decrease from top to bottom. The subsurface topography of this part is rough.

The second layer with resistivity ranges 25 to 94 Ohm- m is expected to be the response of the saturated tuff. The thickness of this layer is 9m with some discontinuities at a distance from 55 to 155m.

The third layer at depth from 15 to 18.4m has the high resistivity range as the first layer with resistivity of 100 to 528 Ohm-m with its resistivity decrease upward from the bottom. The lithological unit of the layer is weathered and fractured scoracious basalt.

II. Dipole-Dipole resistivity inverse model section for Profile-2

The inverse resistivity section of this profile-2 shows nearly the same features with that of profile one except very high resistivity concentrated only on the eastern side of the section as shown in Figure 5.5. Accordingly, the first layer resistivity ranges from 126 to 622 Ohm-m with thickness of about 6m. At distance of about 80m and 170m there are weak zones (discontinuity).and the lithological description of the layer is dry pumice.

The second layer resistivity ranges from 38 to 125 Ohm-m with thickness of 9m and the layer is interpreted in terms of lithology as saturated tuff. The third layer has resistivity range of 180 to 417 Ohm-m with thickness of about 3m and the layer is interpreted in terms of lithology as weathered and fractured scoracious basalt. The resistivity of the first layer decrease downward and that of third layer upward. The broken lines on the two profiles indicate or show discontinuity zones.

5.1.2 Magnetic survey

The results of the magnetic survey were compiled in the form of different maps which have been generated after the field raw data have undergone through different mathematical corrections and filtering using Geosoft software. The results of all magnetic anomaly maps (total, residual, regional anomaly maps) included in the present work are discussed in the following pages.

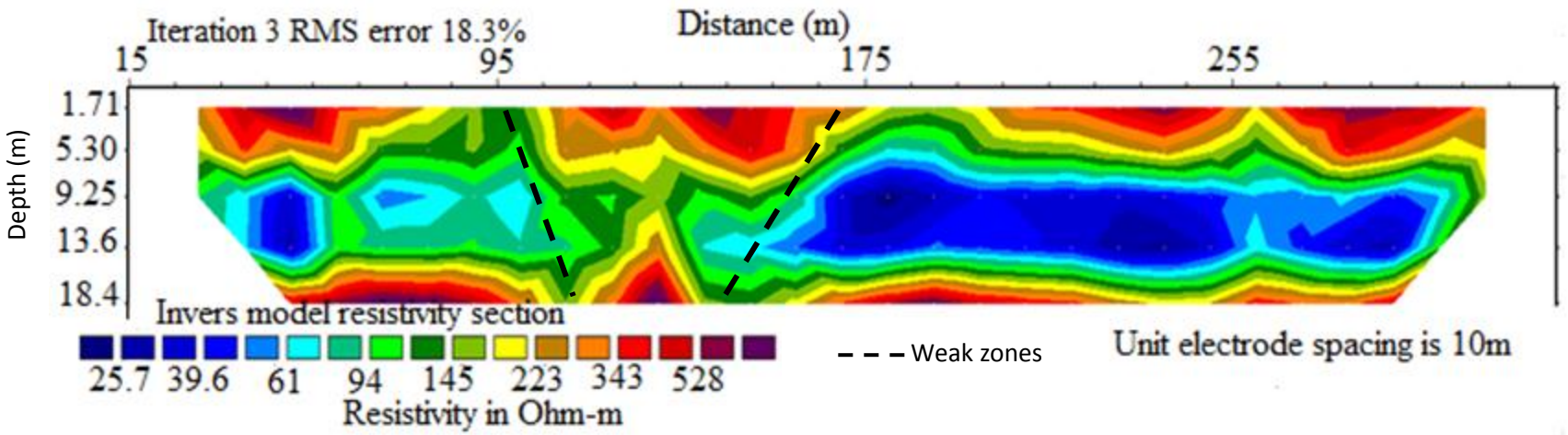

Figure 5.4.2D Electrical resistivity cross section of Profile 1, Oine Chafo Umbure ground fissure, Shashamane.

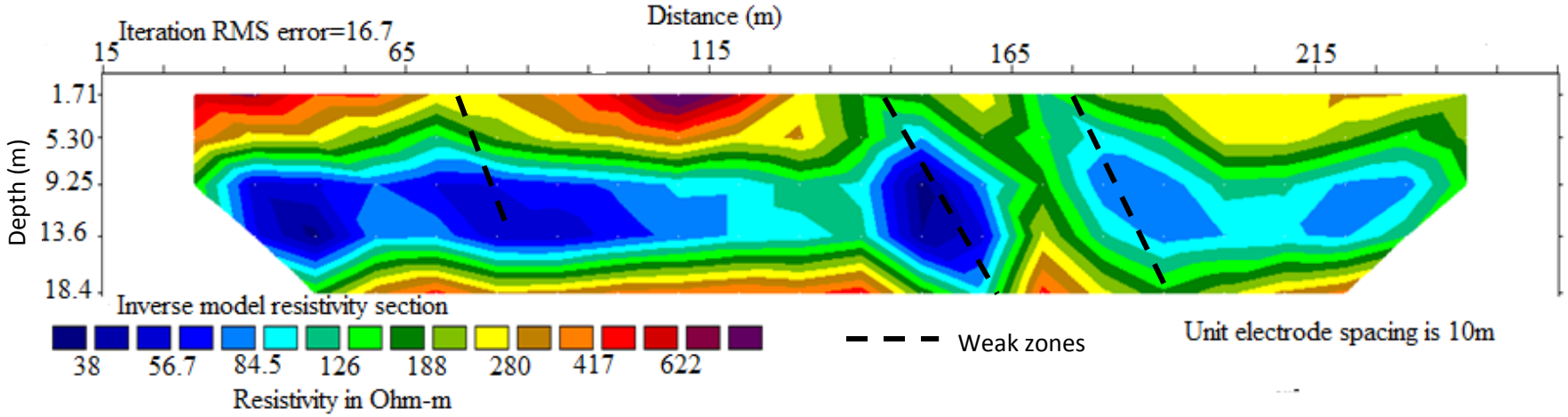

Figure 5.5.2D Electrical resistivity cross section of Profile 2, Oine Chafo Umbure ground fissure, Shashamane.

a.Total magnetic field intensity map

The total magnetic field intensity is raw data with out applying any correction or filtering. This map (Fig. 5.6) shows the total magnetic field intensity distributions in the mapped area. It reflects the magnetic effect of deep and shallow sources (total magnetic field measured in the field).

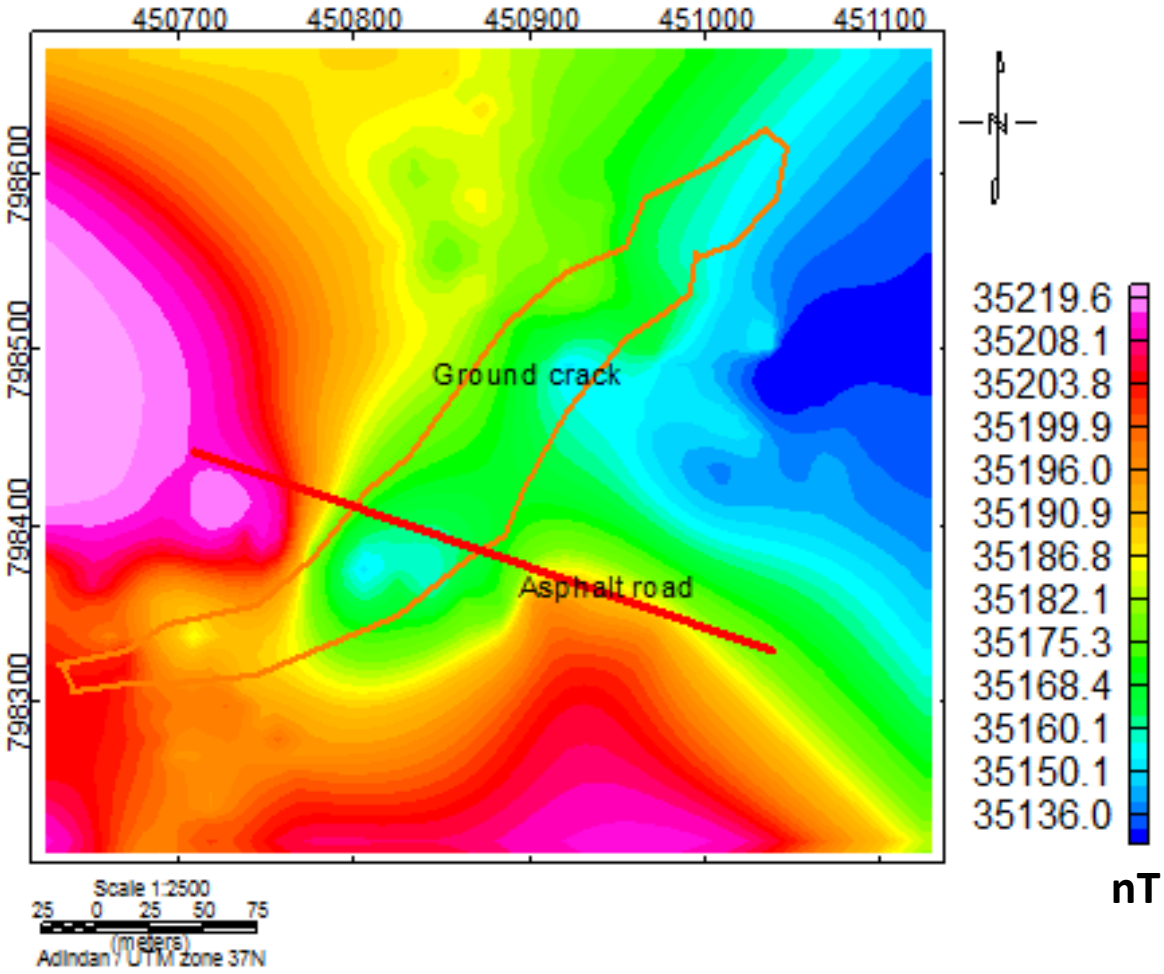

Figure 5.6 Total magnetic field intensity map, Oine Chafo Umbure Ground fissure, Shashamane.

b. Total magnetic field anomaly map

Total magnetic field anomaly is anomalies that have both shallow depth and deeper magnetic field effects. This anomaly map (Figure 5.7), was generated after the field raw data have been corrected for the effects of daily (diurnal) and main (core) field variations (IGRF corrected) in

the earth's magnetic field strength during the course of data acquisition. As maps shows high magnetic field anomalies in the range of greater than 35nT characterize the Western and Southern part of the study area. The lowest magnetic anomaly is observed on the Eastern parts of the study area with value of -32nT and from West to East magnetic anomaly field decreases.

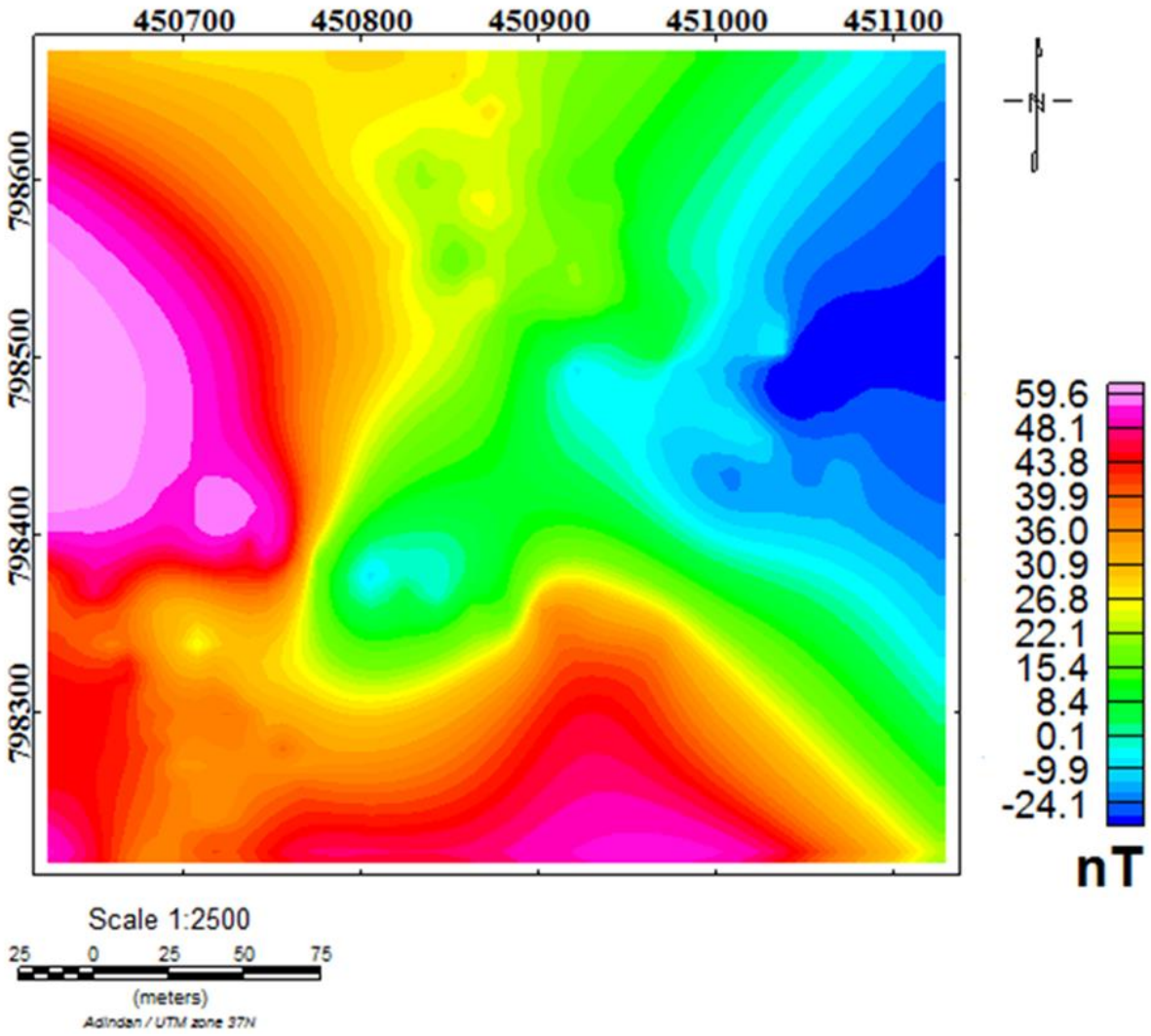

Figure 5.7 Total magnetic field anomaly map, Oine Chafo Umbure ground fissure, Shashamane.

c. Regional magnetic anomaly map

The magnetic anomalies observed over a survey area are gently varying, broad (long wavelength) anomalies known as regional anomalies on which may be superimposed shorter wavelength local anomalies. The regional anomaly may be caused by deep seated large-scale

geologic bodies and the local anomalies by subsurface (shallow) anomalous geologic bodies. The regional anomaly map of the study area was generated by using linear trend analysis method, which is the process of least square fitting to the total anomaly data profile on Microsoft excel and then the trend of least square fitted is calculated by using least square formula that obtained from the fitted line which is the value of regional anomaly (Figure 5.8). The regional magnetic anomaly map shows that the magnetic anomaly decreases from West to East ward with highest magnetic field strength at the east.

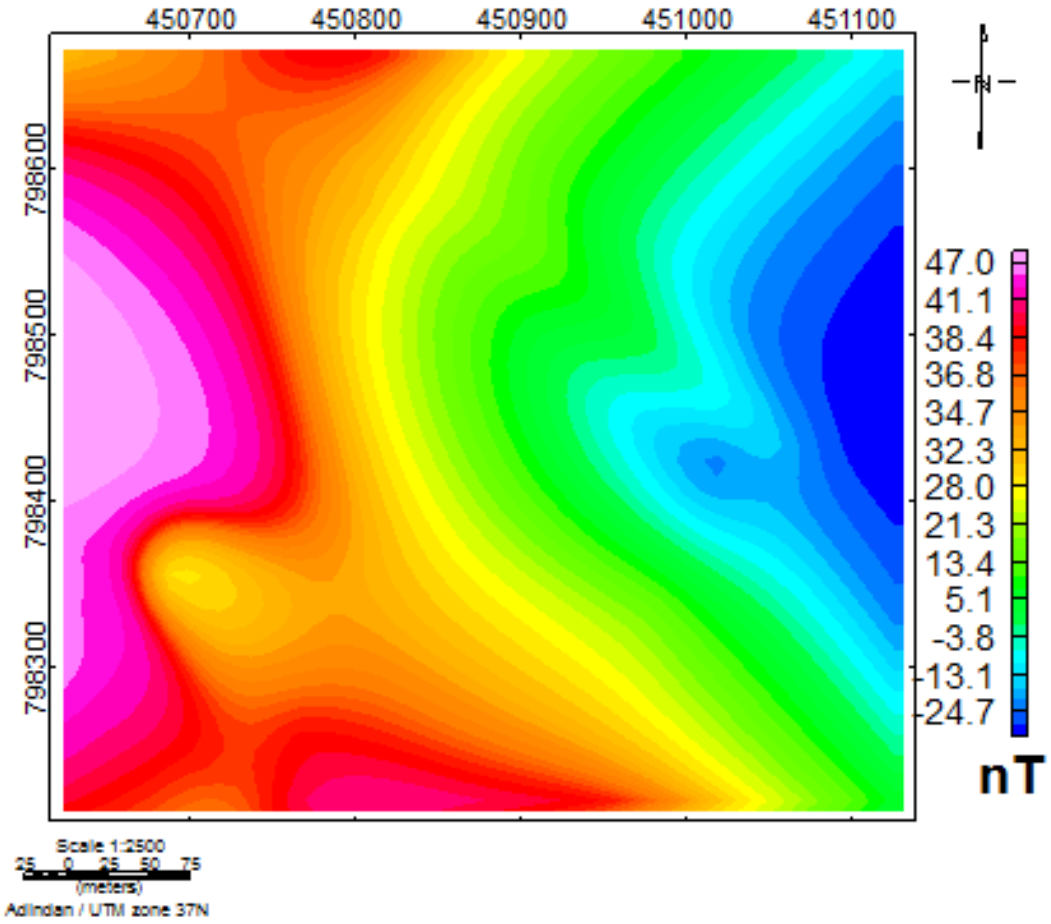

Figure 5.8. Regional magnetic anomaly map, Oine Chafo Umbure ground fissure, Shashamane

d. Residual magnetic anomaly map

The residual magnetic anomaly is anomaly generated due to the shallow depth magnetic field difference in distribution. The residual anomaly map of the study area was generated by

subtracting the calculated leaner trend value (regional anomaly) from the total magnetic anomaly to obtain the residual anomaly and the result contoured by using Geosoft OasisMontaj software (Figure 5.9). The prominent geological features observed in the residual magnetic anomaly map are the low magnetic anomaly that oriented SW to NE and at the northern part. The high magnetic anomaly is located at Eastern and South Eastern parts of the study area.

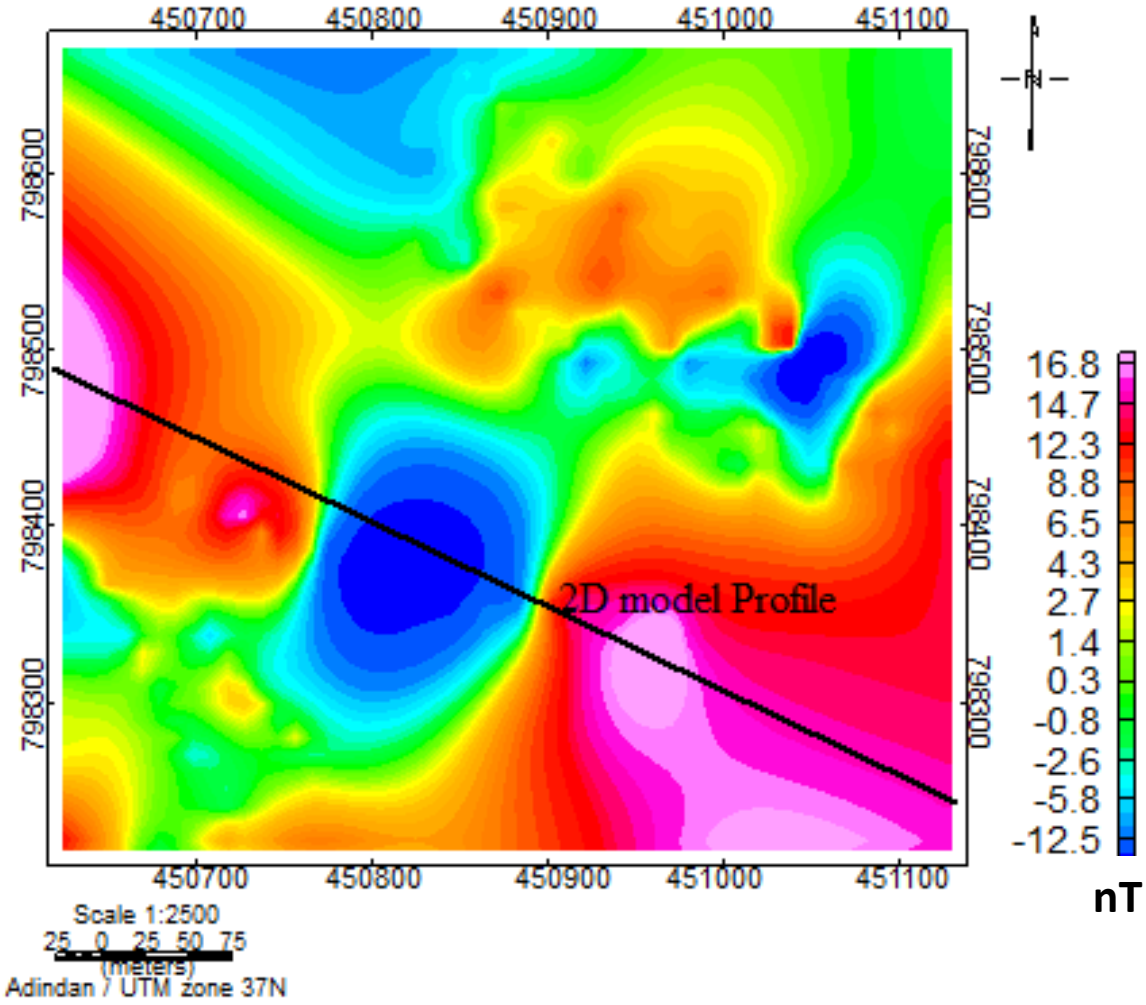

Figure 5.9. Residual magnetic anomaly map, Oine Chafo Umbure Ground fissure, Shashamane

e. Analytic signal map

Analytic-signal maps help to expose the anomaly surface and to highlight discontinuities. It is formed through a combination of horizontal and vertical gradients of a magnetic anomaly. The analytical signal map of the study area is generated after performing analytical enhancement

filtering on the residual magnetic anomaly map. As can be seen from the map (Figure 5.10) with magnetic anomaly highs are observed on the NE, W and central part of the mapped area and a map shows a number of discontinuities that orient approximately NE to SW.

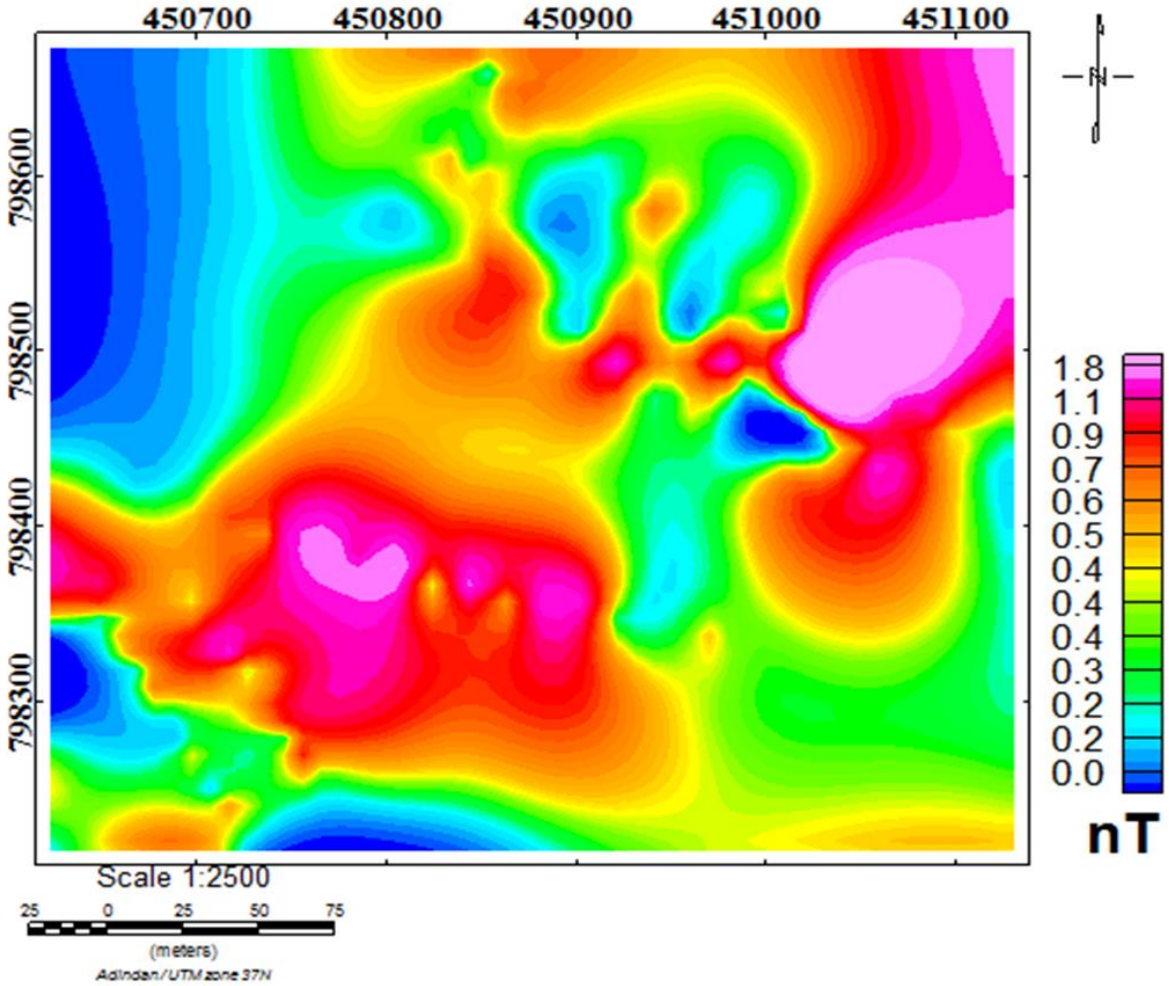

Figure 5.10. Analytic signal magnetic map, Oine Chafo Umbure ground fissure, Shashamane.

f. Magnetic modeled section along Profile 1

Magnetic 2-D modeled section along profile 1 was produced from gridded residual magnetic anomaly data Figure 5.11. The modeled profile is oriented in the NE to SW direction. The 2-D model indicate that the magnetic susceptibility in the area increase downward. At the middle of the profile there is low magnetic susceptibility which shows discontinuities and it is the place where large part of the ground was subducted (asphalt road).

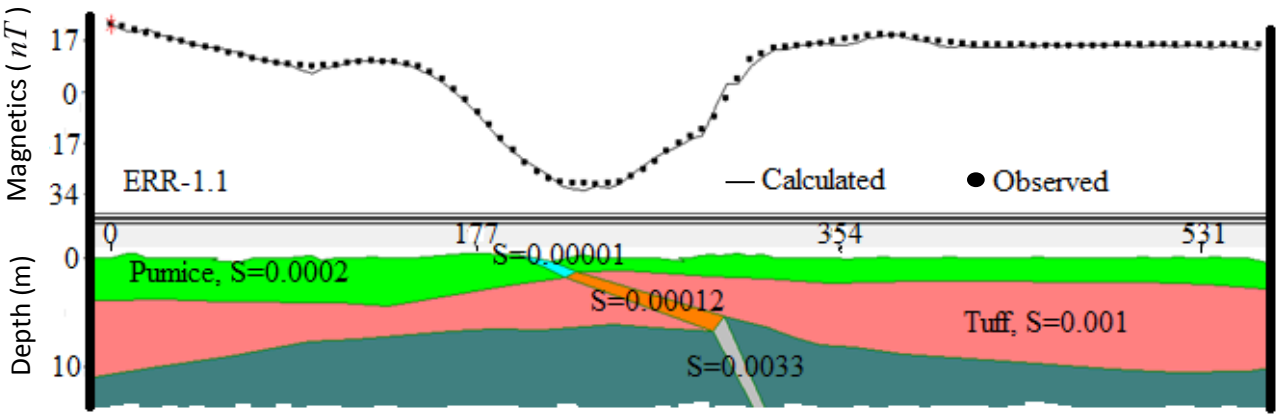

Figure 5.11. The magnetic model section along a selected Profile, Oine Chafo Umbure Ground fissure, Shashamane.

5.2 Conclusions

The work presented the results of integrated geophysical survey that was conducted in the Oine Chafo Umbure, Shashamane, and Central Main Ethiopian rift with the aim to investigate the Ground fissure characteristics. The geophysical methods used are electrical resistivity (VES and Dipole-Dipole profiling) and magnetic methods. The electrical resistivity surveys were conducted by using the IRIS Syscal R1 Plus Swith 72 instrument whereas the magnetic data were collected by an MP 2 Proton Precession Magnetometer. Three (3) Schlumberger array VES point data with (AB/2) max of 500 m and 276 point Axial Dipole-Dipole array data with dipole spacing of 10 m and over 6 depth slices were collected over two profiles. In addition, about 141 point total field magnetic data were collected over six lines. All the acquired data were processed and interpreted qualitatively as well as quantitatively.

The VES data was interpreted qualitatively from the resulting pseudodepth section constructed using the 3 VES data that lie on the survey traverse that runs parallel to the ground fissure. From this section, shallow zone (approximately up to depth of 50m) were found to have high resistivity response corresponding to the lack of moisture in the top part and is underlain by an extensive lower resistivity large part. The VES data were also interpreted quantitatively using the geoelectric section constructed with the layer parameters (depth and resistivity) obtained from interpretation of each VES point data.

The resulting geoelectric section depicts a subsurface consisting of 4 geoelectric horizons. The layer representing the top part of the section shows large variations of resistivity (1240 to 3050 Ohm-m). This thin layer is believed to result from lateral difference in the soil moisture content. Beneath this layer higher resistivity horizon (3727 to 6830 Ohm-m) interpreted to be as the response of dry pumice layer whose thickness extends from a depth of about 1m to 2.5m. The third layer has resistivity range from76 to 111 Ohm-m with thickness of about 9m which is interpreted to be as the response of the saturated tuff. The fourth layer has resistivity range of (375 to 427 Ohm-m) with depth extending beyond 12m. It is interpreted to be the response of weathered and fractured scoraciou basalt.

The Dipole-Dipole resistivity profile data were processed using the RES2DINV software and the results are displayed as 2D inverted model resistivity sections for each profile. The 2D inverse model section of the Profile 1 shows that subsurface consists of three layers on the basis of the resistivity variations. The first layer is characterized by a layer of high resistivity between 100 to 528 Ohm-m with some discontinuity at a distance 95m and 185m and approximately it has a depth of about 6m, interpreted as the response of thick accumulation of dry pumice with its moisture content increasing downward. The subsurface topography of this part is undulating. The second layer whose resistivity ranges from 25 to 94 Ohm-m is expected to be the response of the saturated tuff. The thickness of this layer is about 9m. The third layer found at depths from 15 to about 18m has the near similar resistivity range as that of the first layer with resistivity of 100 to 528 Ohm-m with its moisture content increasing upward.

The 2D inverse model resistivity section of Profile 2, on the other hand, shows nearly the same features with that of Profile 1 except very high resistivity responses concentrated only on the eastern side of the section. Accordingly, the first layer resistivity ranges from 126 to 622 Ohm-m with thickness of 9m. At distance of about 80m and 170m along the traverse are depicted the presence of weak zone (subsurface discontinuity). The second layer resistivity ranges from 38 to 125 Ohm-m with thickness of 9m. The third layer has resistivity range of 126 to 417 Ohm-m with thickness of about 3m.

The residual magnetic anomaly data that was obtained after the linear analysis and separation of regional and residual anomaly from the total magnetic anomaly data is used to interpret the

magnetic data qualitatively. The residual magnetic anomaly map shows that there are two discontinuities (oriented NE to SW that is related to the orientation of the ground fissure and the other one is located at the northern part of the study area). A profile is selected to interpret the magnetic data quantitatively through modeling with the Geosoft Oasis Montaj in terms of 2D model section. The resulting 2D model section shows that there is an extensive discontinuity at the middle of profile corresponding to the large part of Ground is subducted at asphalt road.

In general it has been possible to map the different geoeletrical layers of the subsurface around the Ground fissures and characterize the different underlying formations. It has also been possible to map the presence of subsurface discontinuities extending from the surface to depths that could have been the path ways from the percolation of massive volumes of surface water into the porous second layer (2D model section, magnetic Profile plot and 2D inverse model resistivity sections) to increase the pore pressure and the resulting rupturing of the surface forming the ground fissures.

Based on the above results, regarding the nature of the Oine Chefo Umbure Ground crack and their times of formation, we can possibly conclude:

- The removal of the subsurface pumice by flooding along interconnected different porosity zones may likely be one mechanism for the formation of weak sliding surfaces and ground cracks at the area.
- The orientation of the Ground opening with that of orientation of the major faults within the MER reveals possible tectonic processes that may also strongly favor the formation of the Ground cracks at Oine Chafo Umbure, Shashamane.

5.3 Recommendations

- Although extensive and wide at the surface, from the surveys conducted with the spacing of the electrical surveys, it was not possible to connect the formation of the ground fissures to Rift tectonic structures. Moreover, the surveys conducted were highly confined to the ground fissure and its environs. A deep sounding and magnetic/gravity survey covering a larger area around the fissure is recommended to understand this connection.
- The susceptibility of the area to the formation of ground cracks and resulting damage to property should be considered before planning all developmental initiatives in the area.
- It is recommended that flood canals and drainage routes over the area to be prepared in a way that hydrostatic load from the flood waters is distributed.
- For future settlement and large structure engineering constructions, the foundation of the walls of the houses in the area should be put on compacted subsurface materials.

References

Abebe, T., M. L. Balestrieri and G. Bigazzi (2010). The central Main Ethiopian rift is younger than 8 Ma: confirmation through apatite fission-track thermochronology. *Terra Nova,* **22**(6): 470-476.

Adelusi, A., A. Akinlalu and A. Nwachukwu (2013). Integrated geophysical investigation for post-construction studies of buildings around School of Science area, Federal University of Technology, Akure, Southwestern, Nigeria. *International Journal of Physical Sciences,* **8**(15): 657-669.

Al Fouzan, F. and M. A. Dafalla (2014). Study of cracks and fissures phenomenon in Central Saudi Arabia by applying geotechnical and geophysical techniques. *Arabian Journal of Geosciences,* **7**(3): 1157-1164.

LaikeMariam Asfaw. (1982). Development of earthquake-induced fissures in the Main Ethiopian Rift. *Nature,* **286**, 551–553.

LaikeMariam Asfaw. (1998). Environmental hazard from fissures in the Main Ethiopian Rift. *Journal of African Earth Sciences,* **27**(3-4): 481-490.

Ayalew, L., H. Yamagishi and G. Reik (2004). Ground cracks in Ethiopian Rift Valley: facts and uncertainties. *Engineering geology,* **75**(3): 309-324.

Boccaletti, M., M. Bonini, R. Mazzuoli, B. Abebe, L. Piccardi and L. Tortorici (1998). Quaternary oblique extensional tectonics in the Ethiopian Rift (Horn of Africa). *Tectonophysics,* **287**(1): 97-116.

Boccaletti, M., M. Bonini, R. Mazzuoli and T. Trua (1999). Pliocene-Quaternary volcanism and faulting in the northern Main Ethiopian Rift (with two geological maps at scale 1: 50,000). *Acta vulcanologica,* **11**: 83-98.

Bonini, M., G. Corti, F. Innocenti, P. Manetti, F. Mazzarini, T. Abebe and Z. Pecskay (2005). Evolution of the Main Ethiopian Rift in the frame of Afar and Kenya rifts propagation. *Tectonics,* **24**(1):1-21.

Corti, G. (2009). Continental rift evolution: from rift initiation to incipient break-up in the Main Ethiopian Rift, East Africa. *Earth-Science Reviews,* **96**(1): 1-53.

Kearey, P., M. Brooks and I. Hill (2013). *An introduction to geophysical exploration*, John Wiley & Sons, pp.160-200.

Keranen, K. and S. Klemperer (2008). Discontinuous and diachronous evolution of the Main Ethiopian Rift: Implications for development of continental rifts. *Earth and Planetary Science Letters*, **265**(1): 96-111.

Keir, D., C. J. Ebinger, G. W. Stuart, E. Daly, and A. Ayele (2006), Strain accommodation by magmatism and faulting as rifting proceeds to breakup: Seismicity of the northern Ethiopian rift, *J. Geophys. Res.*, **111**, B05314, doi:10.1029/2005JB003748.

Kim, S., A. A. Nyblade, J. Rhie, C.-E. Baag and T.-S. Kang (2012). Crustal S-wave velocity structure of the Main Ethiopian Rift from ambient noise tomography. *Geophysical Journal International*, **191**(2): 865-878.

Lowrie, W. (2007). *Fundamentals of geophysics*, Cambridge university press, pp. 260-350.

Maguire, P., G. Keller, S. Klemperer, G. Mackenzie, K. Keranen, S. Harder, B. O'reilly, H. Thybo, L. Asfaw and M. Khan (2006). Crustal structure of the northern Main Ethiopian Rift from the EAGLE controlled-source survey; a snapshot of incipient lithospheric break-up. *Geological Society, London, Special Publications*, **259**(1): 269-292.

Muluneh, A. A., M. Cuffaro and C. Doglioni (2014). Left-lateral transtension along the Ethiopian Rift and constrains on the mantle-reference plate motions. *Tectonophysics*, **632**: 21-31.

Reynolds, J. M. (2011). *An introduction to applied and environmental geophysics*, John Wiley & Sons, pp.117-180.

Shemelis, F. (2006). Hydrogeological system analysis in ziway–shala lakes area using hydrochemistry and isotope techniques, central Ethiopia,unpublished MSc. thesis. Addis Ababa University. Addis Ababa, Ethiopia, pp.30-32.

Telford, W. M., L. P. Geldart and R. E. Sheriff (1990). *Applied geophysics*, Cambridge university press, pp.343-560.

Williams, F., M. Williams and F. Aumento (2004). Tensional fissures and crustal extension rates in the northern part of the Main Ethiopian Rift. *Journal of African Earth Sciences*, **38**(2): 183-197.

Wolfenden, E., C. Ebinger, G. Yirgu, A. Deino and D. Ayalew (2004). Evolution of the northern Main Ethiopian rift: birth of a triple junction. *Earth and Planetary Science Letters*, **224**(1): 213-228.